Distribution Agreement

In presenting this thesis as a partial fulfillment of the requirements for a degree from Emory University, I hereby grant to Emory University and its agents the non-exclusive license to archive, make accessible, and display my thesis in whole or in part in all forms of media, now or hereafter now, including display on the World Wide Web. I understand that I may select some access restrictions as part of the online submission of this thesis. I retain all ownership rights to the copyright of the thesis. I also retain the right to use in future works (such as articles or books) all or part of this thesis.

Ke Pan April 8, 2021

Nigrostriatal Dopamine Terminals in DYT1 Dystonia: a 3D Ultrastructural Analysis in DYT1 Knock-in Mice

by

Ke Pan

Yoland Smith, PhD.

Adviser

Neuroscience and Behavioral Biology

Yoland Smith, PhD

Advisor

Rosa VIllalba, PhD

Committee Member

Ellen Hess

Committee Member

Leah Roesch

Committee Member

2021

Nigrostriatal Dopamine Terminals in DYT1 Dystonia: a 3D Ultrastructural Analysis in DYT1 Knock-in Mice

By

Ke Pan

Yoland Smith, PhD

Advisor

An abstract of

a thesis submitted to the Faculty of Emory College of Arts and Sciences

of Emory University in partial fulfillment

of the requirements of the degree of

Bachelor of Science with Honors

Neuroscience and Behavioral Biology

2021

Abstract

Nigrostriatal Dopamine Terminals in DYT1 Dystonia: a 3D Ultrastructural Analysis in DYT1 Knock-in Mice

By Ke Pan

Importance: This thesis presents results of the very first ultrastructural study of the potential pre-synaptic morphological changes of dopamine terminals in the DYT1 KI mice. We used cutting-edge 3D-Electron Microscopy (EM) reconstruction approach to provide a comprehensive view of neural connections and potential structural changes of dopamine synapses in the striatum of DYT1 KI mice.
Objective: Because the underlying mechanism of the decreased dopamine (DA) release in the striatum of DYT1 mice remains unclear, we propose to study potential ultrastructural changes of nigrostriatal DA synapses that could contribute to the reduced striatal DA neurotransmission in DYT1 KI mice.
Materials and Methods: We did immunohistochemistry on dorsal striatal tissues from the WT and DYT1 KI mice groups. We took EM images of DA terminals labeled via tyrosine hydroxylase (TH) under Single Block Facing/Scanning Electron Microscopic (SBF/SEM). Using the Reconstruct software, we reconstructed 80 TH-immunoreactive (TH-IR) terminals in 2 WT and 2 DYT1 KI mice from which we collected the following data: (1) volume of DA terminals, (2) number and area of post-synaptic densities (PSDs) of DA synapses, (3) number and volume of mitochondria in DA terminals. We also took EM images of DA terminals labeled via dopamine transporter (DAT) immunostaining under Transmission Electron Microscope (TEM). We used images from 7 DAT-immunoreactive (DAT-IR) terminals in WT and in DYT1 KI to measure the surface area of vesicles in DAT-IR DA terminals using *ImageJ* software.
Results: In DYT1 KI mice, (1) while the number and area of PSDs on axo-spinous synapses decreased (t-test, $p=0.00561$), the volume of post-synaptic spines increased (t-test, $p= 0.0075$). Also, (2) the number of mitochondria inside TH-IR terminals increased and was correlated with increased volume of TH-IR terminals. Additionally, we found that (3) the number of axo-axonic appositions increased, and (4) the spine-invaginated DA terminals decreased. Other changes in the volume of DA terminals, number and area of PSDs on axo-spinous synapses, volume of mitochondria, area of vesicles in DA terminals were found, but did not reach statistical significance.
Conclusion and Relevance: Our findings highlight altered axo-spinous synapses and post-synaptic spine morphology, increased number of mitochondria in pre-synaptic DA terminals, and increased incidence of axo-axonic dopamine appositions in the striatum of DYT1 dystonic mice models. These changes might contribute to impaired DA neurotransmission and modulation of other striatal afferents, or serve as compensation for the reduced DA release in the striatum of DYT1 mutant mice.

Nigrostriatal Dopamine Terminals in DYT1 Dystonia: a 3D Ultrastructural Analysis in DYT1 Knock-in Mice

By

Ke Pan

Yoland Smith, PhD.

Advisor

A thesis submitted to the Faculty of Emory College of Arts and Sciences

of Emory University in partial fulfillment

of the requirements of the degree of

Bachelor of Science with Honors

Neuroscience and Behavioral Biology

2021

Acknowledgements

Thanks are due to Jean-Francois Pare and Susan Jenkins for technical assistance.
This work was supported by a grant from the Department of Defense (EH, YS) and the Yerkes Primate Center NIH/ORIP base grant (P51OD01132).
I would like to give special thanks to Dr. Yoland Smith and Dr. Rosa Villalba, for taking me into the field of research and helping me with this project along the way. Thanks to Dr. Ellen Hess, Dr. Leah Roesch for giving me suggestions and supporting me for a better thesis. Thanks to all my lab members for being great mentors. Thanks to my family members, friends, and professors, for shaping me into a better person during my undergraduate years.

Table of Contents

1 Abstract

Importance: This thesis presents results of the very first ultrastructural study of the potential pre-synaptic morphological changes of dopamine terminals in the DYT1 KI mice. We used cutting-edge 3D-Electron Microscopy (EM) reconstruction approach to provide a comprehensive view of neural connections and potential structural changes of dopamine synapses in the striatum of DYT1 KI mice.

Objective: Because the underlying mechanism of the decreased dopamine (DA) release in the striatum of DYT1 mice remains unclear, we propose to study potential ultrastructural changes of nigrostriatal DA synapses that could contribute to the reduced striatal DA neurotransmission in DYT1 KI mice.

Materials and Methods: We did immunohistochemistry on dorsal striatal tissues from the WT and DYT1 KI mice groups. We took EM images of DA terminals labeled via tyrosine hydroxylase (TH) under Single Block Facing/Scanning Electron Microscopic (SBF/SEM). Using the Reconstruct software, we reconstructed 80 TH-immunoreactive (TH-IR) terminals in 2 WT and 2 DYT1 KI mice from which we collected the following data: (1) volume of DA terminals, (2) number and area of post-synaptic densities (PSDs) of DA synapses, (3) number and volume of mitochondria in DA terminals. We also took EM images of DA terminals labeled via dopamine transporter (DAT) immunostaining under Transmission Electron Microscope (TEM). We used images from 7 DAT-immunoreactive (DAT-IR) terminals in WT and in DYT1 KI to measure the surface area of vesicles in DAT-IR DA terminals using ImageJ software.

Results: In DYT1 KI mice, (1) while the number and area of PSDs on axo-spinous synapses decreased (t-test, p=0.00561), the volume of post-synaptic spines increased (t-test, p= 0.0075). Also, (2) the number of mitochondria inside TH-IR terminals increased and was correlated with increased volume of TH-IR terminals. Additionally, we found that (3) the number of axo-axonic appositions increased, and (4) the spine-invaginated DA terminals decreased. Other changes in the volume of DA terminals, number and area of PSDs on axo-spinous synapses, volume of mitochondria, area of vesicles in DA terminals were found, but did not reach statistical significance.

Conclusion and Relevance: Our findings highlight altered axo-spinous synapses and post-synaptic spine morphology, increased number of mitochondria in pre-synaptic DA terminals, and increased incidence of axo-axonic dopamine appositions in the striatum of DYT1 dystonic mice models. These changes might contribute to impaired DA neurotransmission and modulation of other striatal afferents, or serve as compensation for the reduced DA release in the striatum of DYT1 mutant mice.

2 Background and Rationale

2.1 DYT1 Dystonia and DYT1 Dystonic Mice Models

The dystonias are a group of disorders defined by specific types of abnormal movements. Some typical symptoms include sustained, patterned, repetitive muscle contractions, movements that are involuntary and not suppressible, and movements that are task-specific such as writer's cramp (Richter and Richter, 2014; Jinnah and Factor, 2015). DYT1 dystonia, also known as dystonia musculorum deformans and Oppenheim's disease, is a dominantly inherited form of generalized dystonia in which deletion of a single GAG codon in the TOR1A gene results in the loss of a glutamic acid residue in a novel ATP-binding protein (torsinA) (Furukawa et al., 2000).

DYT1 dystonic mice models generally do not exhibit overt dystonic symptoms (Jinnah et al., 2017, Imbriani et al., 2020), but do exhibit some subtle motor abnormalities related to motor learning deficits or poor performance in more challenging motor tests (Dang et al., 2005; Sharma et al., 2005; Shashidharan et al., 2005; Page et al., 2010; Song et al., 2012; Yokoi et al., 2015). Specifically, (1) mice expressing mutated human TOR1A (DYT1 ΔGAG) created by Sharma and colleagues exhibit reduced motor learning ability (Sharma et al., 2005), slightly increased hindlimb step width (Zhao et al., 2008), and reduced spontaneous motor activity (Hewett, 2010). (2) DYT1 ΔGAG transgenic mice created by Shashidharan and colleagues exhibit hindlimb clasping and circling (Shashidharan et al., 2005) and sustained contractions (Chiken et al., 2008). However, subsequent studies doubted these observations since these mice exhibit these phenotypes even in the absence of detectable transgene expressions, indicating that these behaviors may not be attributed to mutant torsinA expression (Giannakopoulou et al., 2010; Richter and Richter 2014). (3) Mice created by Grundmann and colleagues with two-fold

overexpression of DYT1 ΔGAG protein show hyperactivity and decreased learning on the rotarod (Grundmann et al., 2007; Richter and Richter 2014). (4) Striatal and cortex TOR1A knockout (KO) mice created by Li, Yokoi, and colleagues, and TorsinA knockdown (KD) mice, exhibit hyperactivity and motor deficits on beam walking (Dang et al., 2006; Yokoi et al., 2008; Yokoi et al., 2011; Yokoi et al., 2015).

Targeted, or knock-in (KI) mutation of the murine TOR1A (DYT1 ΔGAG KI) created by Goodchild and colleagues (Goodchild et al., 2005), which are the mice used in this study, exhibit hyperactivity, reduced motor skills, and increased foot slips on the beam test (Song et al., 2012). The brain of these DYT1 KI mice appears grossly normal in most dystonic mice models, such as unchanged neuronal cell density in the striatum of DYT1 transgenic mice via Nissl staining (Wang et al., 2016). However, some histological studies have revealed microstructural defects in the striatum of DYT1 transgenic mice (Song et al., 2013; Jinnah et al., 2017; Maltese et al., 2018). For example, the DYT1 ΔGAG heterozygous KI exhibit smaller and less complex spines via Golgi staining (Song et al., 2013). Mutant TOR1A KO mice exhibit sparse and decreased number of D2 receptors in the striatum (D'Angelo et al., 2020). Although it is likely that these mutant mice models undergo structural changes in the striatum, the specific morphological changes of different synapses and cell types require further study.

2.2 Reduced DA Release in DYT1 Mice

A general view is that dystonic disorders are linked with dysfunctional dopamine (DA) neurotransmission. Besides some contradictory results considering DA basal levels, DA turnover (DOPAC: DA ratio, or HVA: DA ratios) (Augood et al., 2002; Dang et al., 2005; Dang et al., 2006; Grundmann et al., 2007; Page et al., 2010; Song et al., 2012; Wang et al., 2016), which are

mostly considered as experimental variance, studies have identified several common neurochemical properties of DYT1 transgenic mice models: reduced brain tissue torsinA level (Goodchild et al., 2005; Yokoi et al., 2010; Yokoi et al., 2015), decreased striatal D2R availability (Augood et al., 2002; Napolitano et al, 2010; Yokoi et al., 2011; Dang et al., 2012; Zhang et al., 2015; Bonsi et al., 2019; D'Angelo et al., 2020) and impaired D1R activities (Yokoi et al., 2015; Zhang et al., 2015).

The most prevalently suggested property is impaired amphetamine or electrical stimulated striatal dopamine release via in vivo microdialysis or voltammetry (Sharma et al., 2005; Baicioglu et al., 2007; Page et al., 2010; Song et al., 2012; Imbriani et al., 2020), or reduced DA release by conditional expression of TOR1A (ΔE) in DA neurons (Downs et al., 2020).

How is DA released in the striatum? Although some studies indicated that dopamine functions through volume transmission, in which neurotransmitters diffuse in tissue to activate relatively distant receptors for signaling (Agnati et al., 1995; Rice and Cragg, 2008), a prominent model is that DA transmission is mediated by classical fast synapse-like vesicular exocytosis. Many studies supported this vesicular exocytosis as a releasing mechanism for DA based on several reasons (1) axonal DA varicosities are densely packed with clusters of small, clear vesicles (Yung et al., 1995; Caille et al., 1996; Uchigashima et al., 2015). (2) quantal events (i.e. individual vesicular packets of dopamine) can be recorded using amperometry or whole cell voltage clamp from dopamine axons or cell bodies (Staal et al., 2004; Borisovska et al., 2013; Gantz et al., 2013; Kress et al., 2014). (3) with blockade or knockout of the vesicular monoamine transporter type 2 (VMAT2), dopamine transmission is eliminated (Fon et al., 1997; Tritsch et al., 2012). Additionally, axonal DA release requires active zone-like release sites, because

studies implied that release-ready vesicles containing DA are tethered close to Ca2+ channels, and because DA axons contain active zone-like protein scaffolds (Pan and Ryan, 2012; Liu et al., 2018). Conditional knockout of an important protein scaffold, RIM, largely abolished action potential-triggered DA release (Liu et al., 2018; Liu and Kaeser, 2019).

Under the assumption that DA is released via classical vesicular exocytosis at active zone-like sites, understanding each step of the DA vesicular exocytosis is important for studying potential deficits of striatal DA release. First, DA that is converted from L-DOPA is loaded into vesicles by VMAT2. These vesicles then form the readily releasable pool of neurotransmitter-filled vesicles. Upon terminal depolarization, voltage gated Ca2+ channels open. Ca2+ influxes and initiates vesicle fusion of these neurotransmitter-filled vesicles with the plasma membrane, pore formation, DA release, and vesicle reformation. Once released, DA diffuses from the terminal to activate DA receptors. DA is rapidly taken back up into the presynaptic neurons by the DA transporter (DAT). A host of GPCRs and ligand-gated ion channels further regulate DA synthesis and release (Downs et al., 2020).

Studies have tested potential deficits concerning each step of the DA vesicular exocytosis releasing mechanism to explain this reduced DA release in DYT1 KI mice. (1) as for neurotransmitter packaging, studies have looked at VMAT2 protein. However, results from different studies seem contradictory: while cell lines expressing torsinA(ΔE) had restricted VMAT2 proteins (Misbahuddin et al., 2005), this is not seen in post-mortem human DYT1-TOR1A brains (Walker et al., 2002). (2) as for synaptic vesicle fusion, release, and recycling, studies found that overexpression of torsinA(ΔE) would lead to an abnormal quantity of vesicular fusing proteins (e.g. synaptotagmin-1), enhanced vesicle recycling, and abnormal N

type Ca2+ channel activity, (Pisani et al., 2006; Granata et al., 2008; Martella et al., 2009; Granata et al., 2011; Sciamanna et al., 2011). (3) as for DA reuptake, studies found somewhat contradictory results: while there was reduced membrane-localized DAT or less efficient DAT in Tor1a+/ΔE KI mice (Torres et al., 2004), but studies also found no altered DA clearance in the mutant mice (Page et al., 2010). (4) as for the mediating effect of pre-synaptic receptors onto DA release, D2 DA receptors were found to inhibit DA release (Dwoskin et al., 1986), and nicotinic acetylcholine receptors were found to enhance DA release (Pontieri et al., 1996).

Although there is extensive work on studying the mechanism behind this reduced DA release mechanism in the DYT1 KI mice, most of the studies are pharmacological and present either contradictory or indirect results (without ultrastructural analysis that could visually or graphically demonstrate the morphological changes of pre-synaptic cell structures). One study did some ultrastructural analysis of the synapses in the striatum of DYT1 KI mice and found that axo-dendritic synapses increased, and axo-spinous synapses decreased in the mutant mice (Song et al., 2013). However, this study did not look at potential presynaptic releasing deficits. Additionally, their study was done using single profiles/images of TH immunoreactive terminals and their post-synaptic targets, which partially presented the structural changes in the synapses. It is unknown if the structural changes would be altered via analysis of serial EM images. Thus, more ultrastructural analysis of pre-synaptic and post-synaptic morphological changes presented via serial EM images are needed to provide potential explanations for this reduced striatal DA release in DYT1 KI mice.

2.3 Rationale

Because the underlying mechanism of the decreased DA release in the striatum of DYT1 mice remains unclear, we propose to study potential ultrastructural changes of nigrostriatal DA synapses that could contribute to the reduced striatal DA neurotransmission in DYT1 KI mice.

On one hand, we further studied the potential ultrastructural changes in pre-and post-synaptic elements of DA synapses in the mouse striatum by comparing the ultrastructure of TH-immunoreactive terminals and their post- synaptic targets between control and DYT1 knock-in mice. The following morphometric measurements were collected from the TH-immunoreactive terminals using a three-dimensional electron microscopy reconstruction approach (Single Block Facing/Scanning Electron Microscopic- SBF/SEM) and the Reconstruct (NIH) software: (1) volume of the DA terminals, (2) number and surface area of PSDs, and correspondingly the size and distribution of post-synaptic targets, including post-synaptic dendritic spines, dendritic shafts, and unlabeled terminals/pre-terminal axons, (3) number and volume of mitochondria in the DA terminals.

In addition, we looked at serial ultrathin sections of DAT-immunoreactive dopaminergic terminals in the transmission electron microscope (TEM), compared the (4) size of synaptic vesicles in DAT-immunoreactive dopaminergic terminals between control and DYT1 knock-in mice using the Image J (FIJI, NIH) software.

Our study provided the very first ultrastructural evidence of the potential pre-synaptic morphological changes in the DYT1 KI mice. We also introduced the use of 3D reconstruction to provide a better view of neural connections and potential structural changes.

3 Hypothesis

The overall hypothesis is that the decreased DA neurotransmission in the striatum of DYT1 knock-in mice are caused by pathological ultrastructural plasticity of the presynaptic and postsynaptic structures of dopaminergic synapses.

4 Material and Methods

4.1 Animals

Heterozygous DYT1(ΔE) knock-in mice were maintained congenic with C57BL/6J and genotyped using a PCR-based method (Goodchild et al., 2005). Normal and heterozygous DYT1(ΔE) knock-in mice were tested at 3 months of age. Experiments were performed blindly to genotype. We used 2 mice per group. For the present study, these mice were perfusion-fixed with a mixture of paraformaldehyde (4%) and glutaraldehyde (0.1%). After perfusion, the brains were dissected out from the skull and cut into 50 um-thick coronal sections with a vibrating microtome before being processed for immunocytochemistry.

4.2 Antibodies

Antigen	**Immunogen**	**Species**	**Vendor**	***Dilution***
Tyrosine hydroxylase (TH)	Denatured tyrosine hydroxylase from rat pheochromocytoma (denatured by sodium dodecyl sulfate)	Rabbit	Millipore	1:300
Dopamine transporter (DAT)	Synthetic peptide from the intracellular C-terminal region of human dopamine transporter (CEKDRELVDRGEVRQFTL RHWL)	Rabbit	Chemicon international	1:500

Table 1: Antibodies.

4.3 TH- and DAT-Immunocytochemistry Protocol

Both TH and DAT immunoreactivity were localized with highly specific commercially available antibodies that have been well characterized and heavily used in many laboratories. The Avidin-Biotin Complex (ABC) immunoperoxidase reaction, a procedure routinely used in Dr. Yoland Smith's laboratory, was applied to localize TH in this study. In brief, a series of striatal sections from wildtype and DYT1 mice were incubated overnight with the primary antibody against TH, which were followed by 1-hour incubations in biotinylated secondary antibody reactions and ABC. Then, sections were incubated with the chromogen diaminobenzidine tetrahydrochloride (DAB) to reveal the immunostaining. For DAT immunostaining, striatal sections were incubated overnight at RT with the DAT antibody diluted in Tris-buffered saline (TBS)-gelatin buffer (0.02 M Tris). After rinses with TBS-gelatin, the sections were incubated with goat-anti- rabbit IgGs conjugated with 1.4-nm gold particles (dilution 1:100; Nanoprobes Inc.), then rinsed with TBS-gelatin and transferred to a 1% aqueous sodium acetate solution before the intensification of the gold particles with HQ Silver kit (Nanoprobes Inc.). This tissue was then prepared for electron microscopy.

4.4 Transmission Electronic Microscopy (TEM)

DAT-immunostained striatal sections were postfixed in a 1 % osmium tetroxide solution for 20 min. Following washes in PB, the samples were dehydrated in a stepwise manner in 50–100% alcohol solutions before being placed in propylene oxide. Uranyl acetate (1%) was added to the 70% alcohol to increase contrast in the electron microscope. The dehydrated sections were embedded in epoxy resin (Durcupan, ACM; Fluka, Buchs, Switzerland) for 12 hr, mounted onto oil-coated slides and cover-slipped before being baked at 60°C for 48 hr (Villalba et al., 2016).

Blocks of striatal immunostained tissue were removed from the slides, and glued on top of resin blocks, trimmed and cut into 70-nm ultrathin serial sections (about 9-13 sections on a single grid) with an ultramicrotome (Ultracut T2; Leica, Germany), and collected on single-slot Pioloform-coated copper grids. Ultrathin sections were then stained with lead citrate for 5 minutes and examined with a TEM (JEOL/JEM-1011 electron microscope). Pictures following an entire DAT- immunostained terminal were taken at 75K magnification with a CCD camera (DualView 300W; DigitalMicrograph software, version 2.30.542.0; Gatan, Inc., CA). This material was used to assess the morphology of synaptic vesicles in DA terminals.

4.5 Single Block Facing/Scanning Electron Microscopic (SBF/SEM)

Small regions of TH-immunostained striatal tissue were shipped to Renovo Neural Inc. (Cleveland, OH) in 4% paraformaldehyde for SBF/SEM processing. Series of 200-300 EM images were then obtained from each block of tissue using the SBF/SEM (Zeiss Sigma VP scanning EM, Gatan 3 View in-chamber ultramicrotome). The images were transferred back to us for 3D reconstruction and quantitative ultrastructural analysis of the morphology of DA terminals.

4.6 Ultrastructural 3D Reconstruction (Reconstruct)

Serial digitized electron images of TH-immunoreactive terminals (TIFF formats) were imported into the Reconstruct (NIH) software (http://synapses.clm.utexas.edu/tools/), and individual contours for the immunolabeled terminals, their postsynaptic targets, post-synaptic densities (PSDs), and mitochondria within the terminal were manually traced in each serial electron micrograph. The volumes of TH-positive terminals, the number and volume of their

mitochondria, the number and areas of the PSDs in the post-synaptic structures, the distribution of the postsynaptic dendritic spines, dendritic shafts, and unlabeled terminals/pre-terminal axons, volume of post-synaptic dendritic spines were obtained (50 terminals in each animal).

4.7 Neurotransmitter Vesicle Area (ImageJ)

Serial electron images of entire terminals containing DAT-immunoreactive vesicles were converted into TIFF format, imported into the ImageJ (FIJI, NIH) software (https://imagej.nih.gov/ij/). To avoid overlapping/repetitive tracing of vesicles, sections taken from one terminal were divided into two subsets with subset one containing only odd sections and subset two containing only even sections. In each section, the individual contours for the vesicles were traced and the areas were automatically calculated by the software. The different types of vesicles (round, flat) were manually recognized and noted (232 vesicles from 7 terminals in WT and 237 vesicles from 7 terminals in KI).

4.8 Statistical analysis

The differences between control and DYT1 knock-in mice were statistically assessed using Student's t-test. The inter-individual difference between animals of the same group was tested using one-way ANOVA (Sigmaplot 14.0 software).

5 Results

5.1 Changes in TH-IR terminal sizes between WT and DYT1 KI mice

We used Avidin-Biotin Complex (ABC) immunoperoxidase reaction to localize TH in this study. Since the striatal sections were incubated with the chromogen diaminobenzidine

tetrahydrochloride (DAB) to reveal the immunostaining, the TH immunoreactive (TH-IR) terminals on EM images displayed a darker color compared to unlabeled neurons due to the prevalence of DAB deposits (Figure 1A, B).

We reconstructed a total number of 80 TH-IR terminals in WT and in DYT1 animals using the Reconstruct software (NIH) (Table 2). We found no significant difference in the average volume of TH-IR terminals between WT and KI animals (Figure 1C; 0.375+/-0.0231μm^3 in WT, 0.437+/-0.0239μm^3 in KI; p=0.062). However, when TH-IR terminals were grouped in small- (volume 0.1-0.3μm^3) and large-sized (volume >0.5μm^3) terminals, we found that small-sized TH-IR terminals tended to be slightly more prevalent in WT than in DYT1 mice, while large-sized TH-IR terminals were more abundant in DYT1 mice (Figure 1D).

WT	**KI**
EH13: N=50	EH16: N=50
RM131: N=30	RM135: N=30

Table 2: number of TH-IR terminals analyzed in each animal.

5.2 Morphological changes of TH-IR terminals in DYT1 KI mice

Consistent with previous electron microscopy studies (Arluison et al., 1984; Freund et al., 1984; Smith et al. 1994), we did observe that over 80% of striatal TH-IR terminals were small vesicle-filled enlargements that contain one or two mitochondria and form symmetric synapses with dendrites and spines in the striatum of WT and DYT1 mice (Figure 1A, B). These TH-IR terminals were mostly dispersed in the neuropil between unlabeled cell bodies and bundles of myelinated axons, as previously described (Bouyer et al., 1984).

Additionally, our analysis revealed that there were some TH-IR terminals that had one or multiple spines invaginated into the terminal (Figure 1E). We found a significant decrease in the incidence of spine-invaginated TH-IR terminals in the DYT1 animals compared with WT mice (Figure 1F; 19% in WT, 3% in DYT1).

5.3 Striatal TH-IR synapses in WT vs DYT1 mice

TH-IR terminals formed synapses with two main post-synaptic targets: (1) dendritic shafts (axo-dendritic synapses) and (2) dendritic spines (axo-spinous synapses). Overall, the axo-dendritic and axo-spinous synapses appeared as symmetric synapses with a narrow, short post-synaptic density and a thin synaptic cleft, as described in Arluison et al. (1984) (Figure 2A, B). These synapses were also characterized by the aggregation of synaptic vesicles on the pre-synaptic membrane of the TH-IR terminals. We also found close appositions between TH-IR terminals and unlabeled vesicle-filled terminal- and axon-like profiles. In some cases, these putative axo-axonic contacts exhibited a dark differentiation of pre-synaptic and post-synaptic membrane, as seen in the axo-dendritic and axo-spinous synapses (Figure 7A). However, in most cases, the post-synaptic densities were narrow, short and there was no clear evidence for a synaptic cleft between the two elements, except in a few instances, where synaptic vesicles in one of the profiles were close to the plasma membrane (Figure 7A). For these reasons, we defined these axo-axonic relationships as appositions, instead of synapses, in our study.

The PSDs associated with all TH-IR synapses were discontinuous and short (Figure 2A, B). There was no difference observed in the number of axo-dendritic synapses formed by TH-IR terminals between WT and DYT1 mice (Figure 3C), while there was a decrease in the number of axo-spinous synapses (Figure 3C) and an increase in the number of axo-axonic appositions

(Figure 7; 15 in WT, 35 in DYT1) in the DYT1 mice. There was no significant difference in the mean area of PSDs of axo-dendritic synapses between WT and DYT1 mice, but there was a significant decrease in the mean area of PSDs of axo- spinous synapses in the DYT1 mice (Figure 3B).

Additionally, we noticed that there was a significant increase in the volume of post-synaptic spines targeted by TH-IR terminals in DYT1 mice (Figure 3A).

5.4 Changes in the Number of Mitochondria in TH-IR Terminals of DYT1 mice

The morphology (round or oval-shaped) and volume of mitochondria in TH-IR terminals was comparable between WT and DYT1 mice (Figure 4A, B; Figure 5C). The total number of mitochondria decreased in DYT1 mice (106 mitochondria in WT vs 86 mitochondria in DYT1). Individual TH-IR terminals contained a variable number of mitochondria. To determine if there was a change in the number of TH-IR terminals based on their mitochondria content, we categorized the TH-IR terminals into three groups. Most TH-IR terminals contained 1 mitochondrion in both WT and DYT1 mice (58% in WT, 66% in DYT1). A comparable percentage of TH-IR terminals contained 2 mitochondria between the two groups (25% in WT, 18% in DYT1). However, while 10% of TH-IR terminals contained 3 mitochondria in DYT1 mice, none of the 80 TH-IR terminals reconstructed in WT mice contained 3 mitochondria. There was also a decrease in the percentage of TH-IR terminals that were devoid of mitochondria in DYT1 mice (17% in WT, 6% in KI).

Additionally, we studied the correlation between the volume of TH-IR terminals and the number of mitochondria contained in such terminals. We found that in DYT1 KI mice, as the

size of the terminal increases, the number of mitochondria increases (Figure 5B), emphasizing the importance of mitochondrial activity. Such correlation was not seen in the WT animals (Figure 5A).

5.5 Synaptic vesicles analysis: no difference in the size of synaptic vesicles in DAT-IR terminals between WT and DYT1 KI mice.

Besides analysis of TH-IR terminals, we analyzed potential changes in the size of synaptic vesicles in DAT-IR terminals using high power views of labeled terminals taken with a transmission electron microscope. Since the striatal sections were incubated with antibodies conjugated with 1.4-nm gold particles, the labeled DAT-IR terminals contained 5-6 dark gold particles close to or on the plasma membrane of the terminals (Figure 6A, B). From these terminals, the size of randomly chosen vesicles with an intact membrane was measured. The surface area of a total of 232 vesicles from 7 DAT-IR terminals in WT and 237 vesicles from 7 DAT-IR terminals in DYT1 mice was measured. In general, the vesicles inside DAT-IR terminals were round or oval in shape (Figure 6A, B). There was no difference found between the mean area of vesicles between WT and DYT1 mice (Figure 6C; 487nm^2 in WT, 499nm^2 in DYT1).

6 Discussion

In this study, we hypothesized that the decreased DA neurotransmission in the striatum of DYT1 knock-in mice is caused by pathological ultrastructural changes of the presynaptic and postsynaptic structures of dopaminergic synapses. To test this hypothesis, we used the SBF/SEM approach and the Reconstruct software to reconstruct TH-IR terminals in the striatum of WT and

DYT1 KI mice. From these reconstructed terminals, we compared the following ultrastructural features between the two groups of mice: (1) volume of the terminals, (2) number and surface area of PSDs on synapses between DA terminals and dendritic spines and dendritic shafts, (3) number and volume of mitochondria in the DA terminals, (4) size of synaptic vesicles in the DA terminals. Overall, we found that there was no significant difference in the volume of DA terminals and in the number and surface area of PSDs on axo-dendritic synapses between WT and DYT1 KI mice. However, the number and surface area of PSDs on axo-spinous synapses decreased significantly in KI mice compared with controls. Although axo-axonic synapses could not be convincingly established, we found an increase in the number of axo-axonic appositions between TH-IR terminals and unlabeled terminal- or axon-like profiles in the DYT1 mice. There was no significant difference in the volume of mitochondria in the DA terminals between WT and DYT1 mice, but the number of mitochondria contained in each DA terminal increased in DYT1 mice. No significant difference was found in the surface area of synaptic vesicles in the DA terminals between WT and DYT1 mice. An increase in the volume of post-synaptic spines contacted by TH-IR terminals was found in the DYT1 mice. Also, there was a significant decrease in the number of spine-invaginated TH-IR terminals in the DYT1 mice.

Overall, our findings suggest that the decrease in DA release seen in the DYT1 KI mice models are not due to major ultrastructural changes in the morphology and synaptic architecture of axo-dendritic synapses formed by DA terminals. We did observe some changes in the number and surface area of PSDs of axo-spinous synapses, number of axo-axonic appositions, and number of mitochondria contained in each DA terminal. In addition, changes in the volume of post-synaptic spines and in the number of spine-invaginated TH-IR terminals were found between the two groups. Future studies are needed to determine if these structural changes

account for altered dopamine release or physiological properties of dopamine synapses in DYT1 mice.

6.1 Morphological changes of TH-IR terminals might indicate compensation for reduced DA release

In this study, we assume that the majority of TH-immunoreactive fibers and terminals in the dorsal striatum originate from nigrostriatal neurons which use dopamine as a neurotransmitter and arise from the substantia nigra pars compacta, based on evidence from various sources (Bjorklund and Lindvall, 1984; Parent, 1986, 1990; Gerfen et al., 1987; Smith et al., 1994). The nigrostriatal DA system in mammals, especially in primates, is important for sensorimotor learning via modulation of cortical afferents in the striatum, and its dysfunction or degeneration is strongly associated with movement disorders and neurodegenerative diseases such as dystonia, tics, Tourette syndrome and Parkinson's Disease (Aosaki et al., 1994; Matsumoto et al., 1999).

Recent studies have demonstrated that axonal DA release in the striatum requires active zone-like release sites, which are generally located at the terminal portion of these nigrostriatal DA neurons (Liu et al., 2016; Liu and Kaeser, 2019). These vesicle-filled boutons of dopamine axons are called varicosities and have been described in a number of immunohistochemical studies as being relatively small in size and oblong in shape (Yung et al., 1995; Caille et al., 1996; Descarries et al., 1996). One of the goals of our study was to determine if changes of these structural features are observed in DYT1 mice.

Previous studies have reported contradictory results concerning the morphological changes of nigrostriatal dopamine neurons in dystonic animals or patients. On one hand, there was no

structural abnormalities identified in TH-IR cell bodies or their striatal projections in one DRD dystonia patient (Rajput et al., 1994), and the development of nigrostriatal dopaminergic projections seemed to be normal via light microscope in DYT1 mice (Goodchild et al., 2005). On the other hand, the DYT1 mutant mice were found to show subtle nigrostriatal structural abnormality: specifically, there was a small reduction in the number of TH-IR substantia nigra cells, and the remaining cells were larger than controls. These changes were limited to the substantia nigra and not seen in ventral tegmental TH-IR neurons (Song et al., 2012). Three DYT1 human brains collected at autopsy were reported to give subjective impressions of enlarged nigral neurons without obvious cell loss (Rostasy et al., 2003).

Our results showing subtle, but not significant, enlargement of TH-IR terminals in the DYT1 mutant mice (Figure 1A, B) is consistent with previous studies (Rostasy et al., 2003; Song et al., 2013). While these enlargements might reflect a pathological process, it may also reflect a compensatory mechanism to rescue the decrease in DA release. For example, enlarged DA terminals may be associated with an increased size and number of active zone-like release sites, which might allow the transmission of more synaptic vesicles and thus neurotransmitters such as DA.

Although we didn't quantify the number of TH-IR terminals in our material, it is unlikely that the subtle changes in the number of TH-IR terminals reported in other studies would be sufficient to cause any significant motor deficits. Among different normal mouse strains, the number of midbrain dopamine neurons vary naturally by nearly 2-fold (Zaborszky and Vadasz, 2001). Thus, these subtle changes in the number of TH-IR terminals might be some natural

experimental variance. Only if the cell loss is substantial could any functionally relevant behavioral change be observed (Song et al., 2012).

6.2 Decreased number and area of PSDs on axo-spinous synapses might be associated with reduced DA release

In our study, it was difficult to identify synapses made by these TH-IR terminals because they had a narrow, short post-synaptic density and a thin synaptic cleft, resembling what was seen in Arluison et al (1984).

We are particularly interested in post-synaptic densities, or PSDs, because they contribute to critical features of synaptic integration and regulation. In classical fast synapses, neurotransmitters diffuse across the synaptic cleft to activate clusters of postsynaptic receptors and related protein complexes in the PSDs (Liu and Kaeser, 2019). Thus, PSD plays an important role in neurotransmission by clustering ion channels in the postsynaptic membrane and anchoring signaling molecules such as kinases and phosphatases at the synapse (Kennedy, 1993; Klauck and Scott, 1995; Ziff et al., 1997). Studies have indicated that PSD size is directly correlated with synaptic strength (Bredt and Nicoll, 2003; Villalba and Smith, 2010; Hodges et al., 2011). For example, overexpression of PSD-95 (a protein concentrated at glutamatergic synapses) in hippocampal neurons can drive maturation of glutamatergic synapses by enhancing postsynaptic clustering and activity of glutamate receptors (El-Husseini et al., 2000). Thus, the morphological changes of PSDs on these dopaminergic synapses might potentially explain the pathological changes in dopamine release observed in DYT1 dystonia.

In this study, we observed that there was a significant decrease in the number and area of PSDs at axo-spinous synapses in DYT1 KI mice (Figure 3B, C). Although no previous studies focused on the size of PSDs and its implications on synaptic plasticity and DA release, data from other brain regions showing that large PSDs are often linked to increased synaptic strength, a decrease in the number and area of PSDs may reduce the strength of synapses between DA terminals and post-synaptic structures. Thus, it is possible that the DA neurotransmission at axo-spinous synapses is impaired in DYT1 KI mice. Specifically, the strength of axo-spinous DA synapses may be reduced because of the lower number of postsynaptic DA receptors and related signaling proteins to activate post-synaptic sensing mechanisms. Future studies are needed to assess the exact impairment in post-synaptic sensing mechanism.

6.3 Increased number of axo-axonic appositions might indicate striatal afferents interplay and modulation of DA release

Besides the morphological changes in PSDs on the axo-spinous synapses, there was an increase in the number of axo-axonic appositions (Figure 7C) between TH-IR terminals and other unlabeled terminals in the DYT1 KI mice. Because many of these contacts did not exhibit clear synaptic differentiation, as seen in the axo-dendritic and axo-spinous synapses, we define them as appositions. In a few cases, vesicles were observed close to the terminal plasma membrane in serial sections suggesting evidence for synaptic contacts, but these were rare. In these cases, DA terminals were either pre-synaptic or post-synaptic to unlabeled vesicle-filled terminals (Figure 7A).

Previous studies have reported incidences or possible existence of axo-axonic synapses formed by DA terminals in the striatum. Some nerve terminals immunoreactive for TH were

found to be in close contact with other nerve terminals in different regions of neostriatum(Arluison et al.,1984). The existence of synaptic contacts between pairs of TH-IR axons were described (Arluison et al.,1984). There was direct apposition of the plasma membranes of the TH-labeled and unlabeled degenerating corticostriatal boutons, suggesting possible axo-axonic interrelationships between two corticostriatal inputs and nigrostriatal inputs (Bouyer et al.,1984). This group also reported that many of the axo-axonic interrelationships between dopaminergic axons and other cortical and possibly non-cortical terminals seemed to occur along the non-varicose portion of the axons (Bouyer et al.,1984).

The striatum mostly receives extrinsic corticostriatal afferents (glutamatergic), nigrostriatal afferents (dopaminergic), thalamostriatal (glutamatergic) afferents, or other GABAergic afferents (Smith and Bolam, 1990), and sometimes receives afferents from intrinsic neurons, including axon collaterals of MSNs and striatal interneurons (Gerfen et al.,1988; Smith et al.,1994; Freund et al.,1984; Nakano et al.,2000; Assous and Tepper, 2018). These striatal afferents make synapses mostly onto striatal MSNs, but they also interplay with each other, which may possibly explain the axo-axonic appositions between these TH-IR fibers and other unlabeled fibers that we are seeing in this study. Understanding the functional significance of these axo-axonic appositions might help to explain the relationship between the increase in these types of axo-axonic synapses and reduced DA release seen in DYT1 KI mice.

Many studies have shed lights on striatal afferents interplay. On one hand, some studies indicated that these nigrostriatal afferents are delivering neurotransmitters and modulating other types of neurons. These could be dopaminergic to glutamatergic axo-axonic synapses, in which nigrostriatal afferents possibly regulate or assist the corticostriatal afferents (Aluison et al.,1984),

or dopaminergic to cholinergic axo-axonic synapses, in which the nigrostriatal dopaminergic afferents are inhibiting striatal cholinergic neurons (Dimova et al.,1993).

On the other hand, studies indicated that nigrostriatal axons and terminals might receive synaptic inputs from other striatal afferents. First, these could be glutamatergic to dopaminergic axo-axonic synapses, which could provide a morphological substrate for the release of DA by L-glutamate (the postulated neurotransmitter in cortical afferents) or glutamate regulation (Bouyer et al.,1984). This possibility is supported by the findings that DA receptors are localized on cerebral cortical afferents to the rat corpus striatum (Schwarcz et al.,1977) and that the activation of DA receptors inhibits calcium-dependent glutamate release from corticostriatal terminals in vitro (Rowlands et al.,1980). Second, another popular view is that of axo-axonic synapses between cholinergic terminals and dopaminergic axons (i.e. striatal cholinergic interneurons to nigrostriatal afferents). A number of recent studies have reported that the activation of striatal cholinergic interneurons elicits local dopamine release from nigrostriatal terminals to support behavioral reinforcement (Cover et al., 2019; Downs et al., 2019). The acetylcholine released by cholinergic interneurons specifically activates nAChRs on dopamine terminals to enhance DA release (Rice and Cragg, 2004; Exley and Cragg, 2008; Threlfell and Cragg, 2011; Downs et al., 2019). Overall, these studies suggest that striatal DA release can be regulated by pre-synaptic modulation. Thus, an increase in axo-axonic contacts might indicate that the release of DA undergoes a stronger cholinergic modulation in the striatum of DYT1 mice than in WT animals.

6.4 Increased number of TH-IR terminals containing more mitochondria might indicate active pre-synaptic mechanism

Mitochondria are closely related to synaptic potentiation. Previous studies utilizing pharmacology to inhibit mitochondria revealed defects in synaptic potentiation and a failure to maintain neurotransmission under rigorous stimulation (Alnaes and Rahamimoff, 1975; Zengel et al., 1994; Tang and Zucker, 1997; Verstreken et al.,2005). Conversely, a fast delivery of mitochondria elicited by tetanic stimulation to the synapse, would facilitate synaptic potentiation (Tong et al., 2007). These findings all suggest an involvement of mitochondria in neurotransmission. Previous studies have proposed a number of possible mechanisms for the modulating role of mitochondria in neurotransmission. For example, Verstreken et al., (2005) hypothesized that the recruitment of reserve pool vesicles depends on mitochondrial ATP production downstream of PKA signaling and that mitochondrial ATP limits myosin-propelled mobilization of reserve pool vesicles.

The changes in the morphology and number of mitochondria are specifically important indicators of mitochondrial functioning. Particularly, in PD animal models, the decreased volume and the increased number of mitochondria in cortical boutons suggest a higher mitochondrial traffic along corticostriatal axons, possibly due to a higher activity and energetic demand at corticostriatal synapses in the parkinsonian condition (Verstreken et al., 2005; Safiulina et al., 2006; Villalba and Smith, 2010).

In our study, we did not observe significant differences in the volume of mitochondria between WT and DYT1 KI (Figure 5C). The morphology of mitochondria was normal, appearing to have the classical “kidney bean” shape. However, we observed a decreased total

number of mitochondria in the DYT1 KI (106 mitochondria in WT, 86 mitochondria in DYT1 KI). Interestingly, while the total number of mitochondria decreased in DYT1 KI, the percentage of TH-IR terminals containing 3 mitochondria increased from 0% to 10%, still indicating possible increased mitochondrial traffic in some TH-IR terminals.

Studies on dystonia reported the role of mitochondria from a more clinical or behavioral perspective. Some studies found mitochondrial DNA or RNA mutation causes dystonic behavioral phenotypes in patients (Sudarsky et al., 1999; Pentelenyi et al., 2009). For example, Pentelenyi et al., (2009) found a novel A8332G heteroplasmic mutation which likely causes dystonia and stroke-like episodes due to mitochondrial encephalopathy. Also, chronic administration of low doses of the complex-II inhibitor 3-nitroproprionic acid (3-NP), which disrupts the mitochondrial respiratory chain and lead to oxidative stress and ATP deficits, does not cause significant motor dysfunction in mice expressing torsinA(δE) (Bode et al., 2012). In fact, Bode et al., (2012) found that the DYT1 mutation protects mice from death caused by 3-NP. These findings suggest that the increased number of TH-IR terminals containing more mitochondria seen in DYT1 mutant mice might serve as some protection from developing dystonic behaviors and pathologies in DYT1 animals. Specifically, with increased mitochondria and correspondingly increased energy support, the cells inside pre-synaptic DA terminals might be more active, leading to a more active DA release mechanism. However, the exact mechanism of how the mitochondria activity interacts with DA release needs further exploration.

6.5 No changes in the size of vesicles indicates normal neurotransmitter concentration and quantal size

Studies have indicated that changes in quantal size, which is measured as the smallest post-synaptic depolarization in response to a single vesicle being released, can contribute to synaptic plasticity (Sulzer and Edwards, 2000; Edwards et al., 2007), and that the modulation of quantal size is associated with corresponding changes in vesicle volume (Zhang et al., 1998; Colliver et al., 2000; Pothos et al., 2002; Gong et al., 2003). For example, genetically increased synaptic vesicle size leads to an increase in quantal size (Zhang et al., 1998). Additionally, the number of transmitters in a vesicle can regulate the volume of the vesicle (Colliver et al., 2000). Thus, it is implied that the size of a synaptic vesicle is closely associated with the neurotransmitters it contains and the quantal size. Understanding the changes in the size of synaptic vesicles might help to explain the impaired DA release seen in DYT1 KI mice.

In our study, we observed no changes in the size of synaptic vesicles in the DA terminals (Figure 6C). Thus, it is possible that the synaptic vesicles contain similar number of neurotransmitters between WT and DYT1 KI. Also, these vesicles might have similar quantal size, meaning that the post-synaptic depolarization in response to a single vesicle being release is similar. This further implies that the vesicle releasing mechanism between WT and DYT1 KI should be similar. If so, the impaired DA release in DYT1 KI mice probably could not be explained by changes in the size of synaptic vesicles in pre-synaptic nigrostriatal DA terminals.

6.6 Increased post-synaptic spine volume might serve as a rescue for reduced DA neurotransmission

Dendritic spines are vulnerable to structural changes during aging and in neurologic diseases (Parajuli et al., 2020). In the striatum, dendritic spines of MSNs are an essential site of information processing from glutamate and dopamine afferents both in physiological conditions and in neurodegenerative events. The size of dendritic spine heads reflects synaptic strength, thus indicating that a significant modification in spine head diameter influences neuronal plasticity (Vastagh et al., 2012).

In our study, we observed an interesting inverse relationship between the number of axo-spinous synapses (consequently the number of PSDs on such synapses) and the volume of post-synaptic spines (i.e. the volume of post-synaptic spines increased as the number of PSDs on axo-spinous synapses decreased) in the striatum of DYT1 KI mice (Figure 3A).

This inverse relationship was reported multiple times in previous studies. While studies found an overall decrease of dendritic spine density in the striatum of DYT1 mutant mice (Song et al., 2013; Maltese et al., 2018; Cai et al., 2021), they also indicated an increased number of mushroom-type spines (Maltese et al., 2018; Cai et al., 2021), or thin spines (Maltese et al., 2018). There are some subtle contradictions among these studies: for example, while Maltese et al., (2018) found a concomitant overall increase of dendritic spine width, Cai et al., (2021) didn't observe significant differences for dendritic spine head width. However, it is still promising that a significant modification in spine morphology might serve as an indicator for the dysfunctional dopamine transmission in the striatum of DYT1 mutant mice. In the cerebellum of DYT1 KI mice, there was a reduction of spine numbers in the quaternary dendrite branches of cerebellar

Purkinje cells, which indicates reduced input signals from parallel fibers to cerebellar Purkinje cells (Yokoi et al., 2012). In PD, reduction in striatal dendritic spine density on MSNs was observed in various rodent models, MPTP-treated monkeys, and PD patients, which is most likely due to the striatal dopamine denervation (Smith et al., 2009; Parajuli et al., 2020). Parajuli et al., (2020) also found that in normal mice, as spine density gradually decreases, the average spine head volume gradually increases with age, suggesting a homeostatic balance between spine head volume and spine density. Overall, these studies confirmed this inverse relationship between dendritic spine density and spine sizes, suggesting a rescue for the reduced synaptic inputs in the mutant animals. Future studies are needed to confirm the specific morphological changes of post-synaptic spines.

6.7 Spine-invaginated terminals indicate more signal and remodeling of neurotransmission in the striatum

In this study, we found a significantly decreased number of spine-invaginated terminals in the DYT1 KI mice (Figure 1E, F). The term “spine-invagination” was first used by Petralia et al., (2015), where they introduced invaginating projections as one of the most striking forms of cellular communication among neurons. Cells may contact other cells via shorter processes that appear to be either irregular varicosities or narrow, elongate structures reminiscent of synaptic spines and called “spinules” (Petralia et al., 2015). While very few studies used the term “invaginating projections”, a number of studies indicated the presence of “synaptic spinules” in the striatum: Boyne and Tarrant (1982) found spinules in synapses of parts of the limbic system of the rat, including the hippocampus, nucleus accumbens, and caudate nucleus (part of the striatum). Perforated synapses with spinules also have been described in the caudate nucleus in

elderly humans (Anglade et al., 1996; Muriel et al., 2001; Petralia et al., 2015). The function of these synaptic spinules is still unclear, but studies found that synaptic spinules might mediate competition between neighboring axons for synapses especially on thin spines (Spacek and Harris, 2004), and that synaptic spinules are induced by high depolarization (electron stimulation) (Tao-Cheng et al., 2009), suggesting that spinules might provide a general mechanism for electric signaling and remodeling of neurotransmission throughout the brain. Thus, a decreased number of spinules potentially indicates inadequate signaling and remodeling of neurotransmission. Since there were fewer spine-invaginating projections in the striatum of DYT1 KI mice, with impaired modulating effects of synaptic spinules, the DA neurotransmission might be limited compared to controls,

Additionally, fewer spine-invaginated terminals might be interpreted as a simplification of spine structures, meaning that the spine morphology is not as complex. In vivo, spines have dynamically changing morphologies that may appear short and stubby, long and thin, or with distal swellings or bifurcations (Bonhoeffer and Yuste, 2002; Fiala et al., 2002; Harris and Kater, 1994). However, in the DYT1 mutants, spines were reported to appear relatively shorter and less complex (Song et al.,2013). Although the functional significance of changes in spine morphology and synaptic connectivity remains unknown, simplification of dendrite and spine structure seems to be a pathological feature commonly found in numerous neurological and psychiatric diseases (Fiala et al., 2002), and is believed to underlie profound intellectual disability in fragile-X syndrome and other mental retardation syndromes where overt degeneration is lacking (Irwin et al., 2000; Von Bohlen Und Halbach, 2010). In DYT1 dystonia, the significant decrease in spine-invaginating projections might at least suggest some alterations

in the spine morphology, and correspondingly alterations in the transmission, integration and processing of cortical, thalamic and nigral inputs to the striatum of DYT1 mice.

7 Conclusion

Our findings highlight the presence of axo-axonic dopamine synapses, altered axo-spinous synapses and post-synaptic spine morphology, and increased number of mitochondria in pre-synaptic DA terminals in the striatum of DYT1 dystonic mice models. These changes might indicate impaired modulation of DA neurotransmission and other striatal afferents, or serve as protection or compensation for this reduced DA release in the striatum of DYT1 mutant mice. Although there are some subtle changes with the morphology of pre-synaptic TH immunoreactive dopaminergic terminals, it is unlikely that these morphological changes of TH-IR terminals would cause any significant behavioral phenotypes. Future studies are needed to explore some unclear details and lingering questions such as (1) specific morphological changes of the spine (spine head, spine neck, categorization of post-synaptic spines e.g. mushroom, spinous, etc), (2) specific mitochondrial activity in the pre-synaptic DA terminals, e.g. distance of mitochondria to the synapses, (3) specific morphological changes and activities of the synaptic vesicles (flat or round shape, as well as the distance of the vesicle pools from the synapses, etc.), (4) identification of the pre-/post-synaptic interneurons that are involved the those axo-axonic synapses, (5) other morphological changes that might be related to this reduced DA release: glia wrapping the pre-synaptic DA terminals , etc.

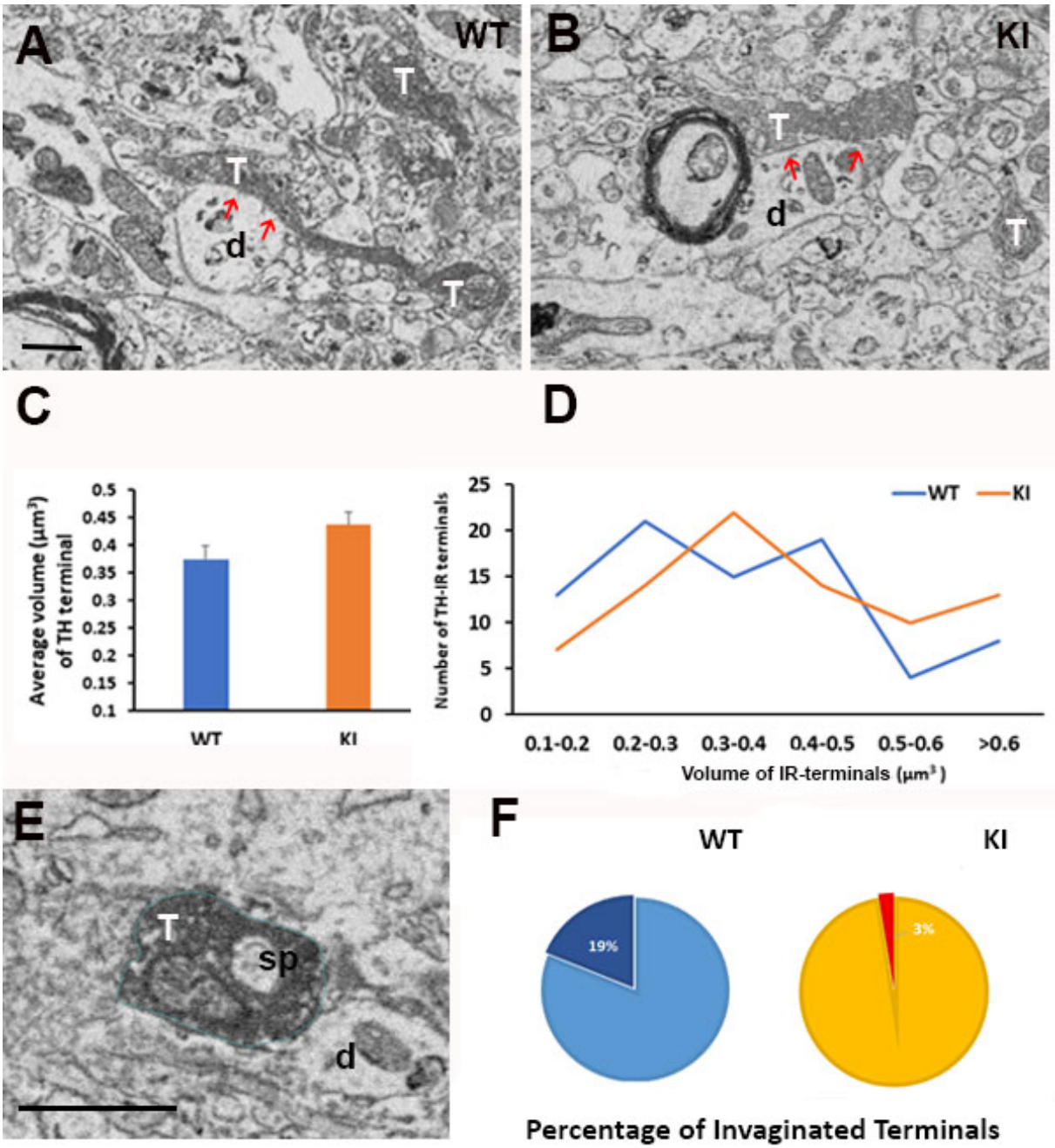

Figure 1: TH-immunoreactive (TH-IR) terminals in the striatum of WT and KI mice. **A and B**: Electron microscope images of TH-IR terminals in the striatum of WT (A) and KI (B). Some of the synaptic contacts between the TH-IR terminals (T) and the dendrites (d) are marked with red arrows. **C**: Histogram showing the comparative analysis of the TH-IR volume in the striatum of WT (n=80) and KI (n=80) mice. The data are expressed as 0.437±0.0239µm^3 in WT and 0.375±0.0231µm^3 in KI mice. The mean volume of the TH-IR terminals was not statistically different between WT and KI mice (T-test analysis, P=0.062). **D**: Volume distribution of the TH-IR terminals in the striatum of WT and KI mice. **E**: Single electron microscope image of a large spine-invaginated TH-IR terminal. **F**: Pie graph comparing the different percentages of spine-invaginated TH-IR terminals between WT (n=15) and KI (n=2) mice. **Abbreviations:** T=TH-IR terminals; d=dendrite; sp=dendritic spine. Scale bar in A (applies to B) and E:500nm

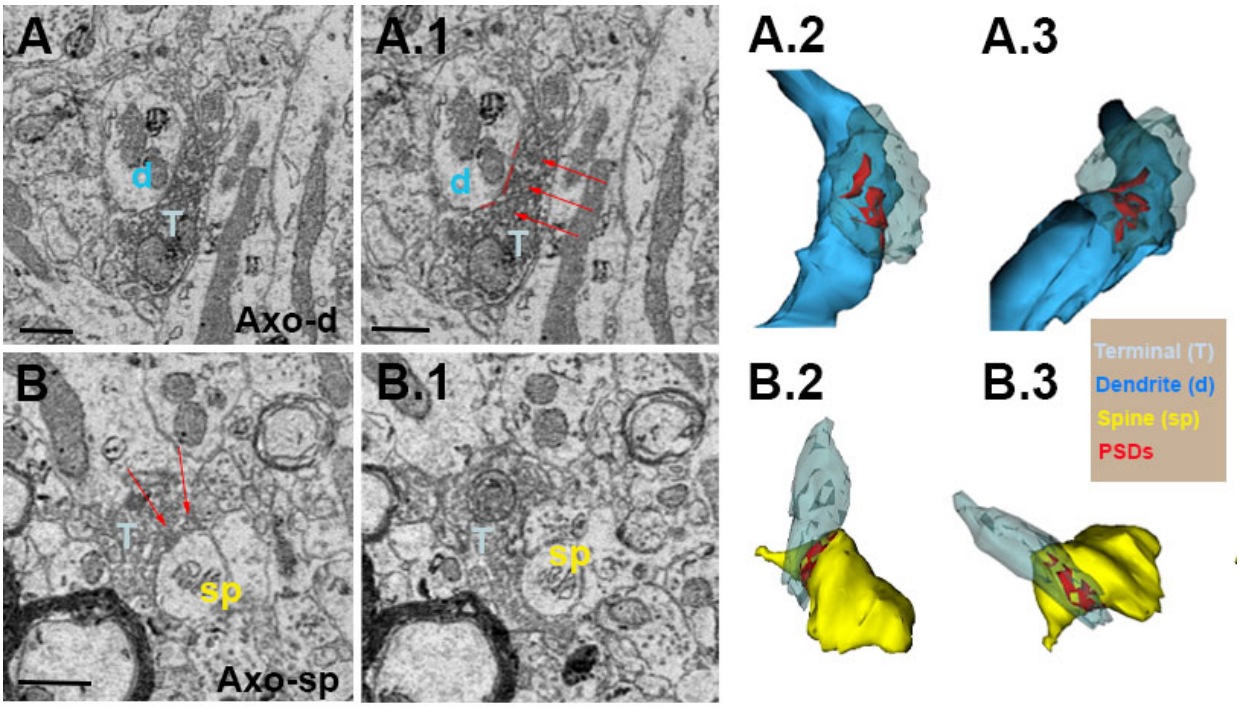

Figure 2: Axo-dendritic and axo-spine synapses of striatal dopaminergic terminals. **A and A.1**: Single electron image of a TH-IR terminal (T) forming a synapse with a dendrite (d). The post-synaptic densities (PSDs) are traced in red in A.1 and indicated with red arrows. **A.2 and A.3:** Two rotated views of the 3D model obtained after the complete reconstruction of the TH-IR terminal shown in A and A.1, and the synaptic contact with the dendrite (d). B and B.1: Serial electron micrographs of a TH-IR terminal (T) forming a synaptic contact with a dendritic spine (sp). The red arrows in B indicate the post-synaptic density. **B.2 and B.3**: Two spatial and rotated views of the 3D model obtained with the serial images and the complete reconstruction of the axo-spine synapse. All these images correspond to KI mice. Scale bar in A, A.1 and B (applies to B.1):500nm

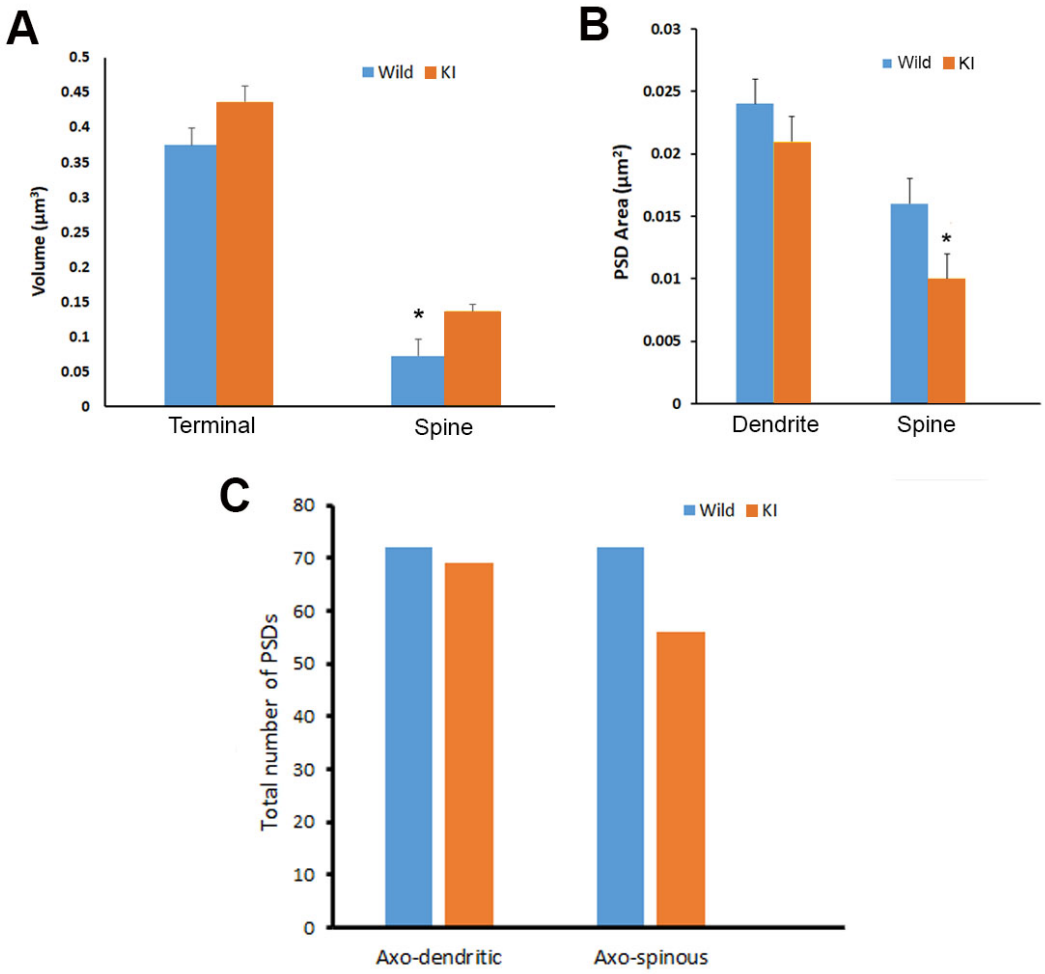

Figure 3: Quantitative analysis of the TH-IR terminals and their synaptic contacts. **A and B**: Histograms comparing the volume (A) of the terminals, spines and the post-synaptic densities (PSDs, B) of the axo-dendritic and axo-spine synapses in the striatum of the WT and KI mice. The data are expressed as $0.0734\pm0.00983\mu m^3$ in WT, and $0.137\pm0.00234\mu m^3$ in DYT1 KI for the volume of post-synaptic spines; $0.0242\pm0.00170\mu m^2$ in WT, $0.0207\pm0.00179\mu m^2$ in DYT1 KI for PSDs on axo-dendritic synapses; $0.0156\pm0.00145\mu m^2$ in WT, $0.00960\pm0.00154\mu m^2$ in DYT1 KI for PSDs on axo-spinous synapses. In the axo-spine synapses of the KI mice, there is a significant increase in the volume of post-synaptic spines and a decrease in the PSD area (T-test, P= 0.0075 and P=0.00561). **C**: Diagram bar comparing the total number of PSDs counted in the axo-dendritic vs the axo-spine synapses in WT and KI mice.

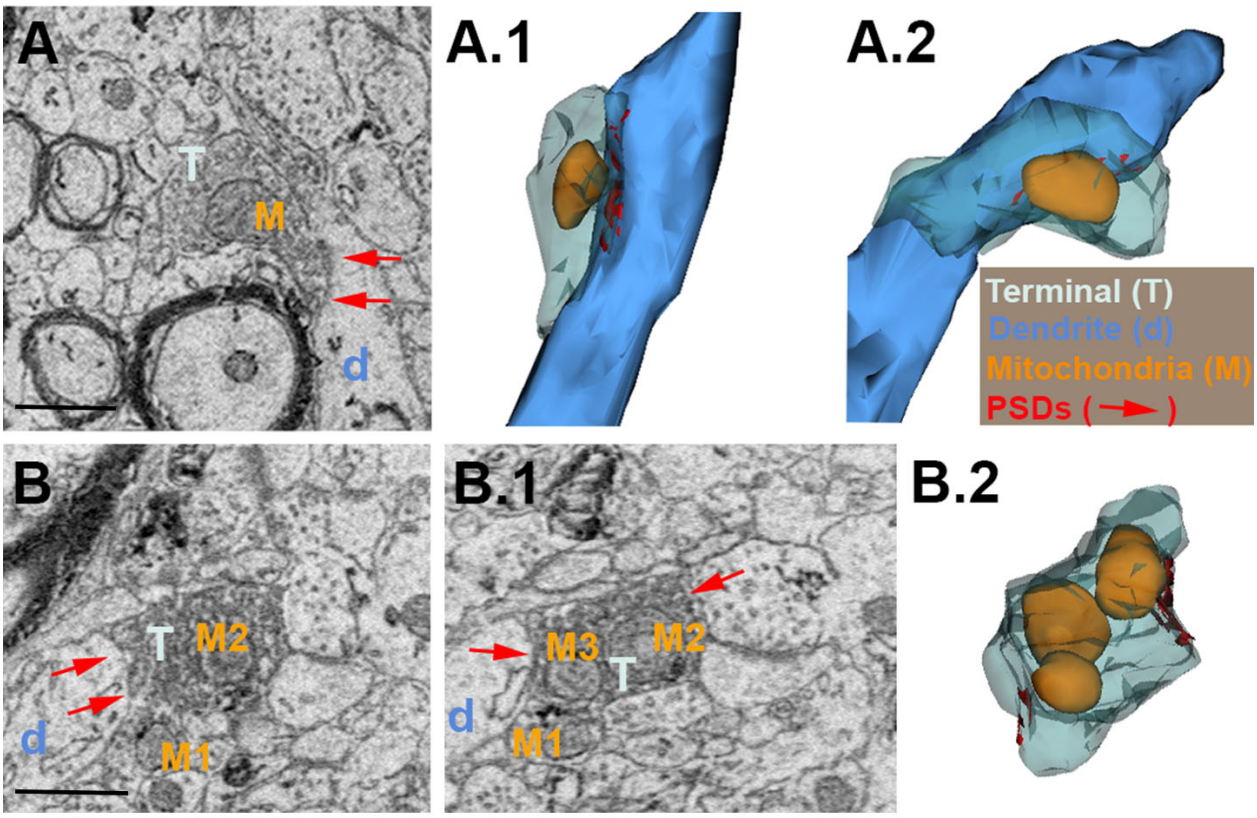

Figure 4: Mitochondria in the TH-IR terminals. **A**: Electron micrograph of a TH-IR terminal (T) containing one mitochondria (M) forming a synaptic contact (red arrows) with a dendrite (d). **A.1 and A.2**: Rotated views of the 3D reconstructed terminal (T), the mitochondria and the post-synaptic densities (PSDs). **B and B.1**: Serial images of a TH-IR terminal forming an axo-dendritic synapse. Notice that in B the number of mitochondria profiles is two (M1 and M2), while in the serial image of the same terminal (B.1) the number of mitochondria profiles is three (M1-M3). **B.2**: 3D model of the complete reconstructed terminal and the mitochondria. The complete reconstruction allows to obtain the unequivocal number of mitochondria in the terminal. Scale bar in A and B (applies to B.1):500nm.

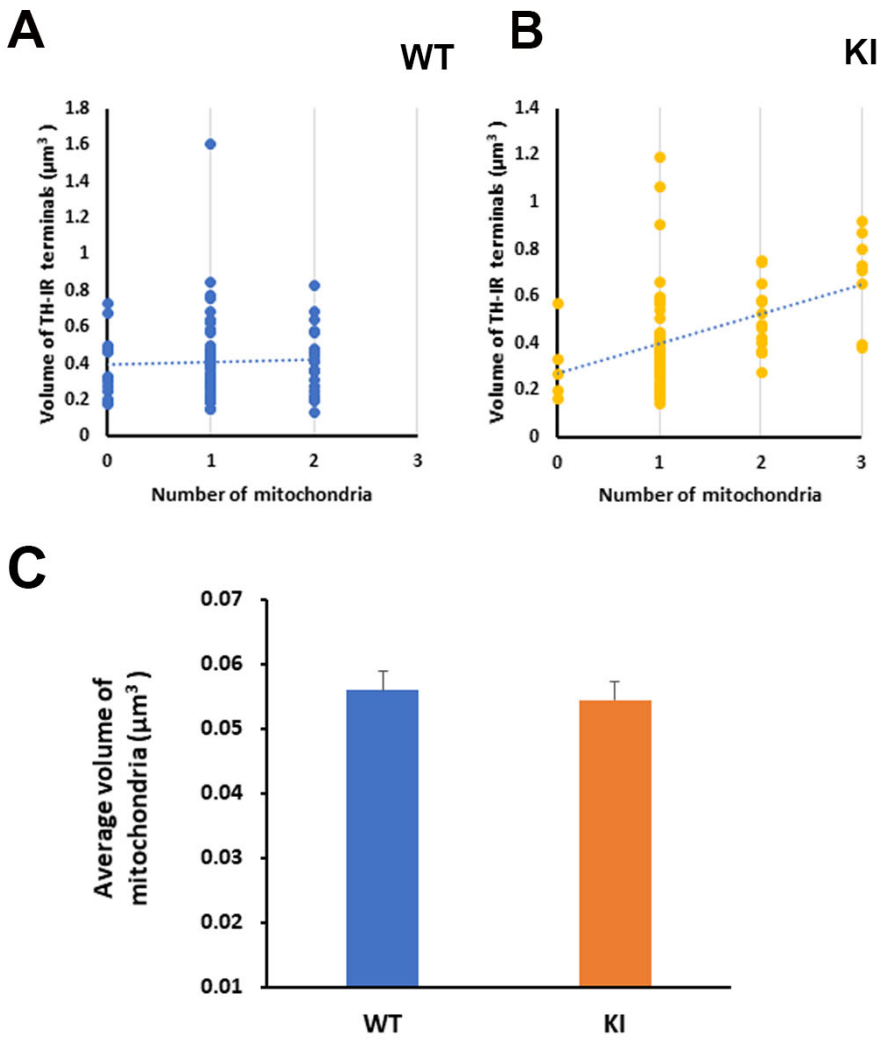

Figure 5: Quantitative analysis of mitochondria. **A and B**: Correlation analysis of the number of mitochondria and the volume of the TH-IR terminals in the WT (A) and KI (B) mice (R^2 =0.001 on WT, R^2=0.1963 in DYT1 KI mice). C: Histogram comparing the average volume of mitochondria in the TH-IR terminals in the WT and KI mice. The data are expressed as 0.0559±0.00318µm^3 in WT, and 0.0544±0.00294µm^3 in DYT1 KI mice. The differences were not statistically significant (T-test, P=0.724)

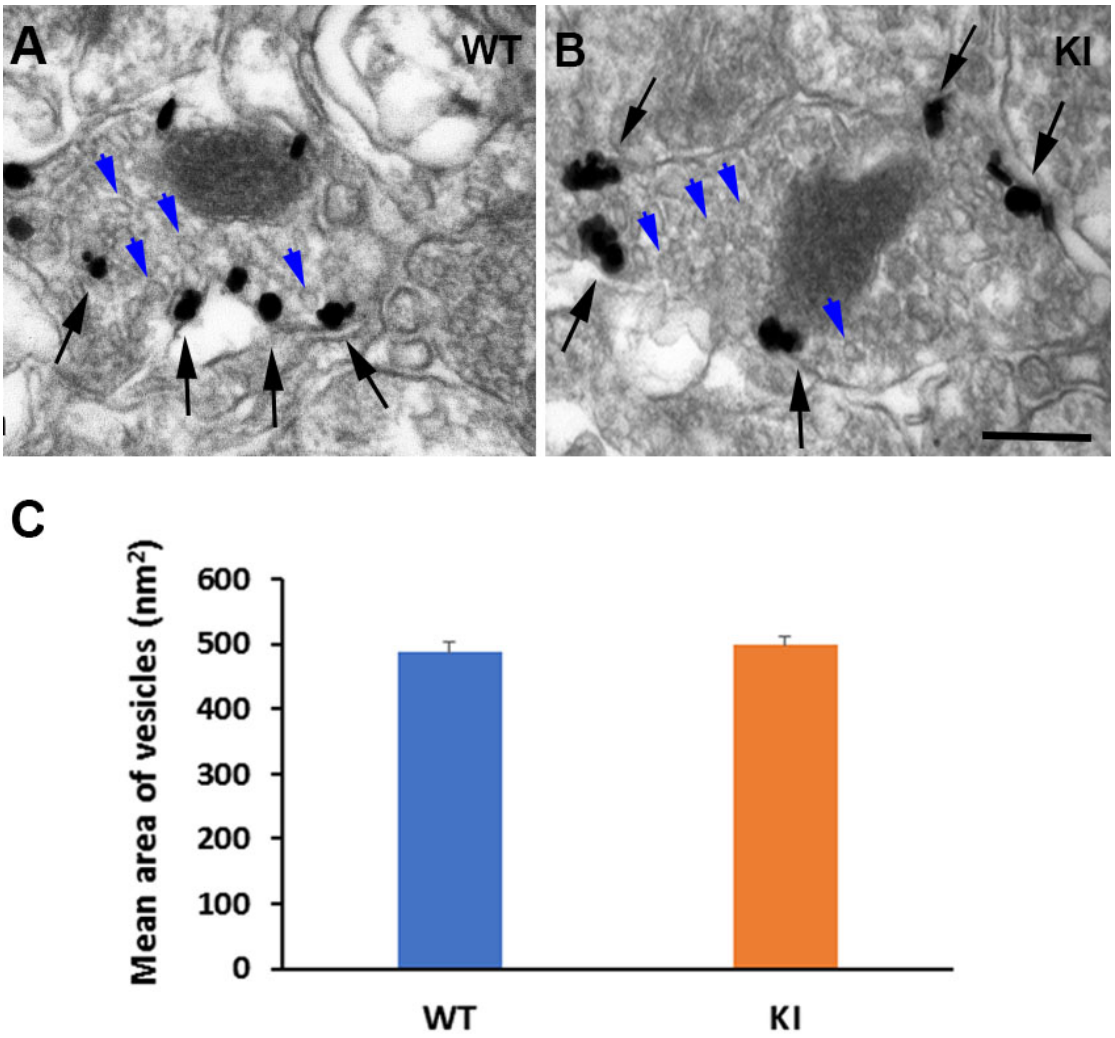

Figure 6: Analysis of the vesicle size in the DAT-immunoreactive terminals. **A and B**: Electron microscope images of DAT-IR terminals (gold immunostaining/silver intensification). The gold particles (black arrows) are associated to the membrane of the dopaminergic terminals. Some of the dopaminergic vesicles in the terminal are indicated with blue arrowheads. **C**: Histogram comparing the size of the neurotransmitter vesicles in the striatal dopaminergic terminals of the WT and KI mice. There are no significant differences in the size of the vesicles (T-test analysis; P=0.57). Values are expressed as 487.428±17.089nm^2 in WT, 499.311±12.178nm^2 in DYT1 KI mice. Scale bar in B (applies to A): 200nm

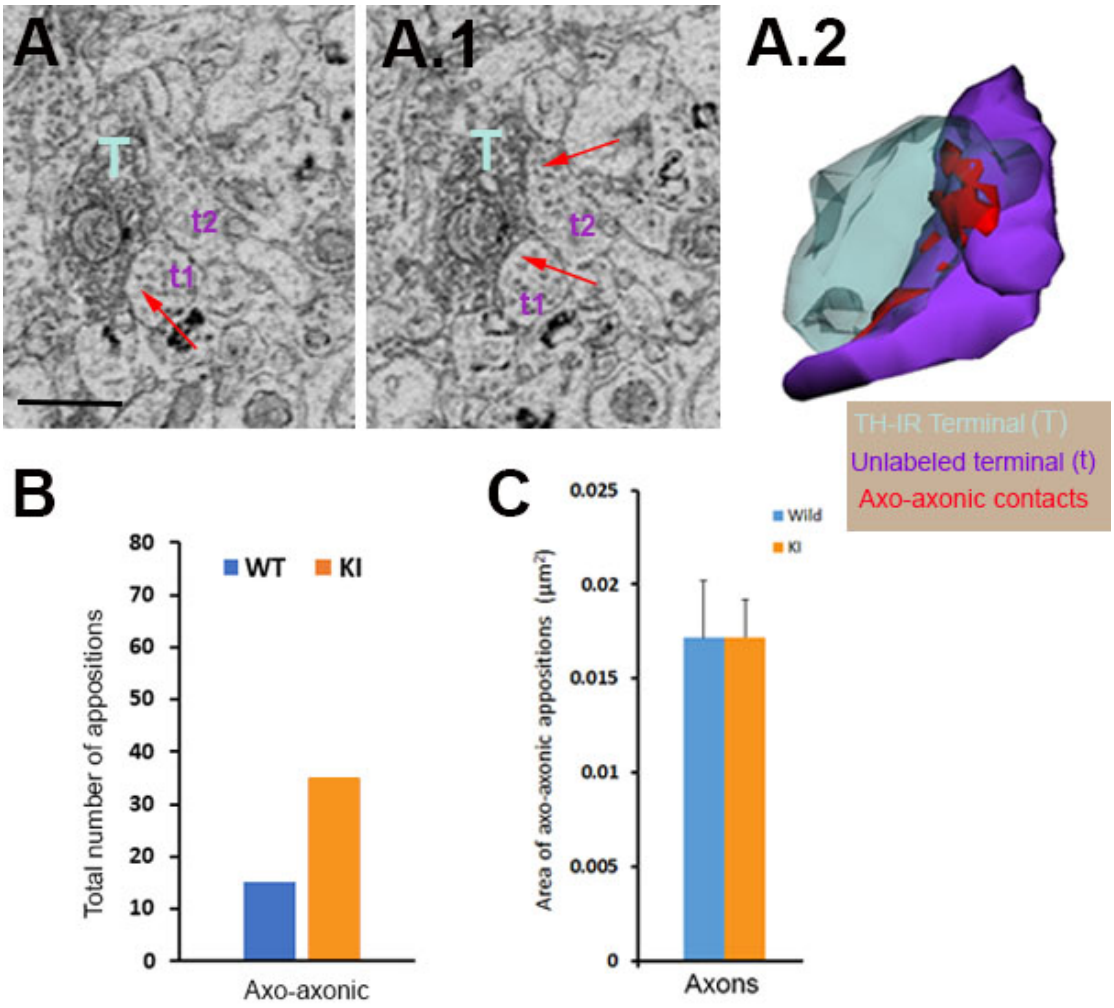

Figure 7: Axo-axonic contacts of TH-IR terminals. **A and A.1**: Serial electron micrographs of a TH-IR terminal (T) contacting with two axons/preterminal axons (t1 and t2). The red arrows indicate the contacting areas of the dopaminergic terminal with t1 and t2. **A.2**: 3D model of the complete reconstruction of the TH-IR terminal, the two terminals/pre-terminals and their contacting areas. **B and C**: Histograms comparing the total number of appositions/axo-axonic contacts (B) and the average area of the appositions (C) in WT and KI mice. The differences in the area were not statistically significant (T-test, P=0.972). Scale bar in A (applies to A.1):500nm

References:

Agnati, L. F., Zoli, M., Strömberg, I., & Fuxe, K. (1995). Intercellular communicationin the brain: wiring versus volume transmission. *Neuroscience*, *69*(3), 711-726.

Aosaki, T., Graybiel, A. M., & Kimura, M. (1994). Effect of the nigrostriatal dopamine system on acquired neural responses in the striatum of behaving monkeys. *Science*, *265*(5170), 412-415.

Arluison, M., Dietl, M., & Thibault, J. (1984). Ultrastructural morphology of dopaminergic nerve terminals and synapses in the striatum of the rat using tyrosine hydroxylase immunocytochemistry: a topographical study. *Brainresearch bulletin*, *13*(2), 269-285.

Asanuma, K., Ma, Y., Okulski, J., Dhawan, V., Chaly, T., Carbon, M., ... & Eidelberg, D. (2005). Decreased striatal D2 receptor binding in non-manifesting carriers of the DYT1 dystonia mutation. *Neurology*, *64*(2), 347-349.

Assous, M., & Tepper, J. M. (2019). Excitatory extrinsic afferents to striatal interneurons and interactions with striatal microcircuitry. *European Journal of Neuroscience*, *49*(5), 593-603.

Augood, S. J., Hollingsworth, Z., Albers, D. S., Yang, L., Leung, J. C., Muller, B., ...& Standaert, D. G. (2002). Dopamine transmission in DYT1 dystonia: a biochemical and autoradiographical study. *Neurology*, *59*(3), 445-448.

Balcioglu, A., Kim, M. O., Sharma, N., Cha, J. H., Breakefield, X. O., & Standaert, D. G. (2007). Dopamine release is impaired in a mouse model of DYT1 dystonia. *Journal of neurochemistry*, *102*(3), 783-788.

Beauvais, G., Bode, N. M., Watson, J. L., Wen, H., Glenn, K. A., Kawano, H., ... & Gonzalez-Alegre, P. (2016). Disruption of protein processing in the endoplasmic reticulum of DYT1 knock-in mice implicates novel pathways in dystonia pathogenesis. *Journal of Neuroscience*, *36*(40), 10245-10256.

Betarbet, R., Turner, R., Chockkan, V., DeLong, M. R., Allers, K. A., Walters, J., ...& Greenamyre, J. T. (1997). Dopaminergic neurons intrinsic to the primate striatum. *Journal of Neuroscience*, *17*(17), 6761-6768.

Bode, N., Massey, C., & Gonzalez-Alegre, P. (2012). DYT1 knock-in mice are not sensitized against mitochondrial complex-II inhibition. *PLoS One*, *7*(8), e42644.

Boeckers TM. The postsynaptic density. Cell Tissue Res. 2006 Nov;326(2):409-22. doi: 10.1007/s00441-006-0274-5. Epub 2006 Jul 25. PMID: 16865346.

Bonhoeffer, T., & Yuste, R. (2002). Spine motility: phenomenology, mechanisms, and function. *Neuron*, *35*(6), 1019-1027.

Bonsi, P., Ponterio, G., Vanni, V., Tassone, A., Sciamanna, G., Migliarini, S., ... & Pisani, A. (2019). RGS 9-2 rescues dopamine D2 receptor levels and signaling inDYT 1 dystonia mouse models. *EMBO molecular medicine*, *11*(1), e9283.

Borczyk, M., Śliwińska, M. A., Caly, A., Bernas, T., & Radwanska, K. (2019). Neuronal plasticity affects correlation between the size of dendritic spine and its postsynaptic density. *Scientific reports*, *9*(1), 1-12.

Borisovska, M., Bensen, A. L., Chong, G., & Westbrook, G. L. (2013). Distinct modes of dopamine and GABA release in a dual transmitter neuron. *Journal of Neuroscience*, *33*(5), 1790-1796.

Bouyer, J. J., Park, D. H., Joh, T. H., & Pickel, V. M. (1984). Chemical and structural analysis of the relation between cortical inputs and tyrosine hydroxylase containing terminals in rat neostriatum. *Brain research*, *302*(2), 267-275.

Breakefield, X. O., Blood, A. J., Li, Y., Hallett, M., Hanson, P. I., & Standaert, D. G. (2008). The pathophysiological basis of dystonias. *Nature Reviews Neuroscience*, *9*(3), 222-234.

Bredt, D. S., & Nicoll, R. A. (2003). AMPA receptor trafficking at excitatory synapses. *Neuron*, *40*(2), 361-379.

Cachope, R., & Cheer, J. F. (2014). Local control of striatal dopamine release. *Frontiers in behavioral neuroscience*, *8*, 188.

Cai, H., Ni, L., Hu, X., & Ding, X. (2021). Inhibition of Endoplasmic Reticulum Stress Reverses Synaptic Plasticity Deficits in Striatum of DYT1 Dystonia Mice.

Caille, I., Dumartin, B., & Bloch, B. (1996). Ultrastructural localization of D1 dopamine receptor immunoreactivity in rat striatonigral neurons and its relation with dopaminergic innervation. *Brain research*, *730*(1-2), 17-31.

Chiken, S., Shashidharan, P., & Nambu, A. (2008). Cortically evoked long-lasting inhibition of pallidal neurons in a transgenic mouse model of dystonia. *Journal of Neuroscience*, *28*(51), 13967-13977.

Colliver, T. L., Pyott, S. J., Achalabun, M., & Ewing, A. G. (2000). VMAT-mediated changes in quantal size and vesicular volume. *Journal of Neuroscience*, *20* (14),5276-5282.

Cover, K. K., & Mathur, B. N. (2020). Axo-axonic synapses: Diversity in neural circuit function. *Journal of Comparative Neurology*.

Cserép, C., Pósfai, B., Schwarcz, A. D., & Dénes, Á. (2018). Mitochondrial ultrastructure is coupled to synaptic performance at axonal release sites. *Eneuro*, *5*(1).

D'Angelo, V., Paldino, E., Cardarelli, S., Sorge, R., Fusco, F. R., Biagioni, S., ... & Sancesario, G. (2020). Dystonia: Sparse Synapses for D2 Receptors in Striatum of a DYT1 Knock-out Mouse Model. *International journal of molecularsciences*, *21*(3), 1073.

Dang, M. T., Yokoi, F., Cheetham, C. C., Lu, J., Vo, V., Lovinger, D. M., & Li, Y. (2012). An anticholinergic reverses motor control and corticostriatal LTD deficits in Dyt1 ΔGAG knock-in mice. *Behavioural brain research*, *226*(2), 465-472.

Dang, M. T., Yokoi, F., McNaught, K. S. P., Jengelley, T. A., Jackson, T., Li, J., & Li, Y. (2005). Generation and characterization of Dyt1 ΔGAG knock-in mouse as a model for early-onset dystonia. *Experimental neurology*, *196*(2), 452-463.

Dang, M. T., Yokoi, F., Pence, M. A., & Li, Y. (2006). Motor deficits and hyperactivity in Dyt1 knockdown mice. *Neuroscience research*, *56*(4), 470-474.

DeSimone, J. C., Febo, M., Shukla, P., Ofori, E., Colon-Perez, L. M., Li, Y., & Vaillancourt, D. E. (2016). In vivo imaging reveals impaired connectivity across cortical and subcortical networks in a mouse model of DYT1 dystonia. *Neurobiology of disease*, *95*, 35-45.

Dimova, R., Vuillet, J., Nieoullon, A., & Kerkerian-Le Goff, L. (1993). Ultrastructural features of the choline acetyltransferase-containing neurons and relationships with nigral dopaminergic and cortical afferent pathways in the rat striatum. *Neuroscience*, *53*(4), 1059-1071.

Downs, A. M., Fan, X., Donsante, C., Jinnah, H. A., & Hess, E. J. (2019). Trihexyphenidyl rescues the deficit in dopamine neurotransmission in a mouse model of DYT1 dystonia. *Neurobiology of disease*, *125*, 115-122.

Downs, A. M., Fan, X., Kadakia, R., Donsante, Y., Jinnah, H. A., & Hess, E. J. (2020). Cell-intrinsic effects of TorsinA (ΔE) disrupt dopamine release in amouse model of DYT1-TOR1A dystonia. *bioRxiv*.

Ebrahimi, S., & Okabe, S. (2014). Structural dynamics of dendritic spines: molecular composition, geometry and functional regulation. *Biochimica et Biophysica Acta(BBA)-Biomembranes*, *1838*(10), 2391-2398.

Edwards, R. H. (2007). The neurotransmitter cycle and quantal size. *Neuron*, *55*(6),835-858.

El-Husseini, A. E. D., Schnell, E., Chetkovich, D. M., Nicoll, R. A., & Bredt, D. S. (2000). PSD-95 involvement in maturation of excitatory synapses. *Science*, *290*(5495), 1364-1368.

Fiala, J. C., Spacek, J., & Harris, K. M. (2002). Dendritic spine pathology: cause or consequence of neurological disorders?. *Brain research reviews*, *39*(1), 29-54.

Fon, E. A., Pothos, E. N., Sun, B. C., Killeen, N., Sulzer, D., & Edwards, R. H. (1997). Vesicular transport regulates monoamine storage and release but is not essential for amphetamine action. *Neuron*, *19*(6), 1271-1283.

Freund, T. F., Powell, J. F., & Smith, A. D. (1984). Tyrosine hydroxylase immunoreactive boutons in synaptic contact with identified striatonigral neurons,with particular reference to dendritic spines. *Neuroscience*, *13*(4), 1189-1215.

Gal, A., Pentelenyi, K., Remenyi, V., Pal, Z., Csanyi, B., Tomory, G., ... & Molnar, M. J. (2010). Novel heteroplasmic mutation in the anticodon stem of mitochondrial tRNALys associated with dystonia and stroke-like episodes. *Actaneurologica scandinavica*, *122*(4), 252-256.

Gantz, S. C., Ford, C. P., Neve, K. A., & Williams, J. T. (2011). Loss of Mecp2 in substantia nigra dopamine neurons compromises the nigrostriatal pathway. *Journal of Neuroscience*, *31*(35), 12629-12637.

Gerfen, C. R. (1988). Synaptic organization of the striatum. *Journal of electronmicroscopy technique*, *10*(3), 265-281.

Giannakopoulou, D., Armata, I., Mitsacos, A., Shashidharan, P., & Giompres, P. (2010). Modulation of the basal ganglia dopaminergic system in a transgenic mouse exhibiting dystonia-like features. *Journal of neural transmission*, *117*(12),1401-1409.

Gong, L. W., Hafez, I., de Toledo, G. A., & Lindau, M. (2003). Secretory vesicles membrane area is regulated in tandem with quantal size in chromaffin cells. *Journal of Neuroscience*, *23*(21), 7917-7921.

Goodchild, R. E., Kim, C. E., & Dauer, W. T. (2005). Loss of the dystonia-associated protein torsinA selectively disrupts the neuronal nuclear envelope. *Neuron*, *48*(6),923-932.

Granata, A., Schiavo, G., & Warner, T. T. (2009). TorsinA and dystonia: from nuclear envelope to synapse. *Journal of neurochemistry*, *109*(6), 1596-1609.

Grundmann, K., Reischmann, B., Vanhoutte, G., Hübener, J., Teismann, P., Hauser,T. K., ... & Riess, O. (2007). Overexpression of human wildtype torsinA and human ΔGAG torsinA in a transgenic mouse model causes phenotypic abnormalities. *Neurobiology of disease*, *27*(2), 190-206.

Hamann, M., & Richter, A. (2004). Striatal increase of extracellular dopamine levels during dystonic episodes in a genetic model of paroxysmal dyskinesia. *Neurobiology of disease*, *16*(1), 78-84.

Harris, K., & Kater, S. B. (1994). Dendritic spines: cellular specializations imparting both stability and flexibility to synaptic function. *Annual review of neuroscience*, *17*(1), 341-371.

Hess, E. J. (2016). *Pathomechanisms of Dopamine Dysregulation in DYT1 Dystonia:Targets for Therapeutics*. Emory University Atlanta United States.

Hewett, J., Johansen, P., Sharma, N., Standaert, D., & Balcioglu, A. (2010). Function of dopamine transporter is compromised in DYT1 transgenic animal model invivo. *Journal of neurochemistry*, *113*(1), 228-235.

Hodges, J. L., Newell-Litwa, K., Asmussen, H., Vicente-Manzanares, M., & Horwitz, A. R. (2011). Myosin IIb activity and phosphorylation status determines dendritic spine and post-synaptic density morphology. *PloS one*, *6*(8), e24149.

Ibáñez-Sandoval, O., Tecuapetla, F., Unal, B., Shah, F., Koós, T., & Tepper, J. M. (2010). Electrophysiological and morphological characteristics and synaptic connectivity of tyrosine hydroxylase-expressing neurons in adult mouse striatum. *Journal of Neuroscience*, *30*(20), 6999-7016.

Imbriani, P., Ponterio, G., Tassone, A., Sciamanna, G., El Atiallah, I., Bonsi, P., & Pisani, A. (2020). Models of dystonia: an update. *Journal of neuroscience methods*, 108728.

Irwin, S. A., Galvez, R., & Greenough, W. T. (2000). Dendritic spine structural anomalies in fragile-X mental retardation syndrome. *Cerebral cortex*, *10*(10), 1038-1044.

Ip, C. W., Isaias, I. U., Kusche-Tekin, B. B., Klein, D., Groh, J., O'Leary, A., ... & Volkmann, J. (2016). Tor1a+/-mice develop dystonia-like movements via a striatal dopaminergic dysregulation triggered by peripheral nerve injury. *Actaneuropathologica communications*, *4*(1), 1-14.

Jaunarajs, K. L. E., Scarduzio, M., Ehrlich, M. E., McMahon, L. L., & Standaert, D.G. (2019). Diverse mechanisms lead to common dysfunction of striatal cholinergic interneurons in distinct genetic mouse models of dystonia. *Journal of Neuroscience*, *39*(36), 7195-7205.

Jinnah, H. A., Neychev, V., & Hess, E. J. (2017). The anatomical basis for dystonia:the motor network model. *Tremor and Other Hyperkinetic Movements*, *7*.

Kakazu, Y., Koh, J. Y., Ho, K. D., Gonzalez-Alegre, P., & Harata, N. C. (2012). Synaptic vesicle recycling is enhanced by torsinA that harbors the DYT1 dystonia mutation. *Synapse*, *66*(5), 453-464.

Kawaguchi, Y., Wilson, C. J., Augood, S. J., & Emson, P. C. (1995). Striatal interneurones: chemical, physiological and morphological characterization. *Trends in neurosciences*, *18*(12), 527-535.

Kornhuber, J., & Kornhuber, M. E. (1986). Presynaptic dopaminergic modulation ofcortical input to the striatum. *Life Sciences*, *39*(8), 669-674.

Kozina, E. A., Khakimova, G. R., Khaindrava, V. G., Kucheryanu, V. G., Vorobyeva, N. E., Krasnov, A. N., ... & Ugrumov, M. V. (2014). Tyrosine hydroxylase expression and activity in nigrostriatal dopaminergic neurons of MPTP-treated mice at the presymptomatic and symptomatic stages of parkinsonism. *Journal ofthe neurological sciences*, *340*(1-2), 198-207.

Kress, G. J., Shu, H. J., Yu, A., Taylor, A., Benz, A., Harmon, S., & Mennerick, S. (2014). Fast phasic release properties of dopamine studied with a channel biosensor. *Journal of Neuroscience*, *34*(35), 11792-11802.

Liu, C., & Kaeser, P. S. (2019). Mechanisms and regulation of dopamine release. *Current opinion in neurobiology*, *57*, 46-53.

Liu, C., Kershberg, L., Wang, J., Schneeberger, S., & Kaeser, P. S. (2018). Dopamine secretion is mediated by sparse active zone-like release sites. *Cell*, *172*(4), 706718.

Maltese, M., Stanic, J., Tassone, A., Sciamanna, G., Ponterio, G., Vanni, V., ... & Pisani, A. (2018). Early structural and functional plasticity alterations in a susceptibility period of DYT1 dystonia mouse striatum. *Elife*, *7*, e33331.

Martella, G., Maltese, M., Nisticò, R., Schirinzi, T., Madeo, G., Sciamanna, G., ... & Pisani, A. (2014). Regional specificity of synaptic plasticity deficits in a knock-in mouse model of DYT1 dystonia. *Neurobiology of disease*, *65*, 124-132.

Martella, G., Tassone, A., Sciamanna, G., Platania, P., Cuomo, D., Viscomi, M. T., ...& Pisani, A. (2009). Impairment of bidirectional synaptic plasticity in the striatum of a mouse model of DYT1 dystonia: role of endogenous acetylcholine. *Brain*, *132*(9), 2336-2349.

Matsumoto, N., Hanakawa, T., Maki, S., Graybiel, A. M., & Kimura, M. (1999). Nigrostriatal dopamine system in learning to perform sequential motor tasks in a predictive manner. *Journal of neurophysiology*, *82*(2), 978-998.

Misbahuddin, A., Placzek, M. R., Taanman, J. W., Gschmeissner, S., Schiavo, G., Cooper, J. M., & Warner, T. T. (2005). Mutant torsinA, which causes early-onset primary torsion dystonia, is redistributed to membranous structures enriched in vesicular monoamine transporter in cultured human SH-SY5Y cells. *Movement disorders*, *20*(4), 432-440.

Nakano, K., Kayahara, T., Tsutsumi, T., & Ushiro, H. (2000). Neural circuits and functional organization of the striatum. *Journal of neurology*, *247*(5), V1-V15.

Napolitano, F., Pasqualetti, M., Usiello, A., Santini, E., Pacini, G., Sciamanna, G., ...& Pisani, A. (2010). Dopamine D2 receptor dysfunction is rescued by adenosine A2A receptor antagonism in a model of DYT1 dystonia. *Neurobiology of disease*, *38*(3), 434-445.

Nirenberg, M. J., Vaughan, R. A., Uhl, G. R., Kuhar, M. J., & Pickel, V. M. (1996).The dopamine transporter is localized to dendritic and axonal plasma membranes of nigrostriatal dopaminergic neurons. *Journal of Neuroscience*, *16*(2), 436-447.

Page, M. E., Bao, L., Andre, P., Pelta-Heller, J., Sluzas, E., Gonzalez-Alegre, P., ... & Ehrlich, M. E. (2010). Cell-autonomous alteration of dopaminergic transmission by wild type and mutant (ΔE) TorsinA in transgenic mice. *Neurobiology of disease*, *39*(3), 318-326.

Pan, P. Y., & Ryan, T. A. (2012). Calbindin controls release probability in ventral tegmental area dopamine neurons. *Nature neuroscience*, *15*(6), 813-815.

Pappas, S. S., Darr, K., Holley, S. M., Cepeda, C., Mabrouk, O. S., Wong, J. M. T., ...& Dauer, W. T. (2015). Forebrain deletion of the dystonia protein torsinA causes dystonic-like movements and loss of striatal cholinergic neurons. *Elife*, *4*,e08352.

Parajuli, L. K., Wako, K., Maruo, S., Kakuta, S., Taguchi, T., Ikuno, M., ... & Koike, M. (2020). Developmental changes in dendritic spine morphology in the striatum and their alteration in an A53T α-synuclein transgenic mouse model ofParkinson's disease. *Eneuro*, *7*(4).

Petralia, R. S., Wang, Y. X., Mattson, M. P., & Yao, P. J. (2015). Structure, distribution, and function of neuronal/synaptic spinules and related invaginating projections. *Neuromolecular medicine*, *17*(3), 211-240.

Petralia, R. S., Wang, Y. X., Mattson, M. P., & Yao, P. J. (2016). The diversity of spine synapses in animals. *Neuromolecular medicine*, *18*(4), 497-539.

Petralia, R. S., Wang, Y. X., Mattson, M. P., & Yao, P. J. (2018). Invaginating structures in mammalian synapses. *Frontiers in synaptic neuroscience*, *10*, 4.

Pisani, A., Martella, G., Tscherter, A., Bonsi, P., Sharma, N., Bernardi, G., & Standaert, D. G. (2006). Altered responses to dopaminergic D2 receptoractivation and N-type calcium currents in striatal cholinergic interneurons in amouse model of DYT1 dystonia. *Neurobiology of disease*, *24*(2), 318-325.

Pothos, E. N., Mosharov, E., Liu, K. P., Setlik, W., Haburcak, M., Baldini, G., ... & Sulzer, D. (2002). Stimulation-dependent regulation of the pH, volume and quantal size of bovine and rodent secretory vesicles. *The Journal ofphysiology*, *542*(2), 453-476.

Quartarone, A., & Pisani, A. (2011). Abnormal plasticity in dystonia: disruption of synaptic homeostasis. *Neurobiology of disease*, *42*(2), 162-170.

Radcke, C., Stroh, T., Dworkowski, F., & Veh, R. W. (2002). Specific visualization of precipitated cerium by energy-filtered transmission electron microscopy for detection of alkaline phosphatase in immunoenzymatic double labeling of tyrosine hydroxylase and serotonin in the rat olfactory bulb. *Histochemistry and cell biology*, *118*(6), 459-472.

Rajput, A. H., Gibb, W. R. G., Zhong, X. H., Shannak, K. S., Kish, S., Chang, L. G.,& Hornykiewicz, O. (1994). Dopa-responsive dystonia: pathological and biochemical observations in a case. *Annals of Neurology: Official Journal of the American Neurological Association and the Child Neurology Society*, *35*(4), 396402.

Rice, M. E., & Cragg, S. J. (2008). Dopamine spillover after quantal release:rethinking dopamine transmission in the nigrostriatal pathway. *Brain research reviews*, *58*(2), 303-313.

Richter, F., & Richter, A. (2014). Genetic animal models of dystonia: common features and diversities. *Progress in neurobiology*, *121*, 91-113.

Scarduzio, M., Zimmerman, C. N., Jaunarajs, K. L., Wang, Q., Standaert, D. G., & McMahon, L. L. (2017). Strength of cholinergic tone dictates the polarity of dopamine D2 receptor modulation of striatal cholinergic interneuron excitabilityin DYT1 dystonia. *Experimental neurology*, *295*, 162-175.

Schwarcz, R., Creese, I., Coyle, J. T., & Snyder, S. H. (1978). Dopamine receptors localised on cerebral cortical afferents to rat corpus striatum. *Nature*, *271*(5647),766-768.

Sciamanna, G., Bonsi, P., Tassone, A., Cuomo, D., Tscherter, A., Viscomi, M. T., ...& Pisani, A. (2009). Impaired striatal D2 receptor function leads to enhanced GABA transmission in a mouse model of DYT1 dystonia. *Neurobiology ofdisease*, *34*(1), 133-145.

Sciamanna, G., Hollis, R., Ball, C., Martella, G., Tassone, A., Marshall, A., ... & Standaert, D. G. (2012a). Cholinergic dysregulation produced by selective inactivation of the dystonia-associated protein torsinA. *Neurobiology ofdisease*, *47*(3), 416-427.

Sciamanna, G., Tassone, A., Mandolesi, G., Puglisi, F., Ponterio, G., Martella, G., ...& Pisani, A. (2012b). Cholinergic dysfunction alters synaptic integration between thalamostriatal and corticostriatal inputs in DYT1 dystonia. *Journal of Neuroscience*, *32*(35), 11991-12004.

Segawa, M., Nomura, Y., & Nishiyama, N. (2003). Autosomal dominant guanosine triphosphate cyclohydrolase I deficiency (Segawa disease). *Annals of Neurology:Official Journal of the American Neurological Association and the Child Neurology Society*, *54*(S6), S32-S45.

Sharma, N., Baxter, M. G., Petravicz, J., Bragg, D. C., Schienda, A., Standaert, D. G., & Breakefield, X. O. (2005). Impaired motor learning in mice expressing torsinA with the DYT1 dystonia mutation. *Journal of Neuroscience*, *25*(22), 5351-5355.

Shashidharan, P., Sandu, D., Potla, U., Armata, I. A., Walker, R. H., McNaught, K.S., ... & Olanow, C. W. (2005). Transgenic mouse model of early-onset DYT1 dystonia. *Human molecular genetics*, *14*(1), 125-133.

Silberberg, G., & Bolam, J. P. (2015). Local and afferent synaptic pathways in the striatal microcircuitry. *Current opinion in neurobiology*, *33*, 182-187.

Smith, A. D., & Bolam, J. P. (1990). The neural network of the basal ganglia as revealed by the study of synaptic connections of identified neurons. *Trends inneurosciences*, *13*(7), 259-265.

Smith, Y., & Kieval, J. Z. (2000). Anatomy of the dopamine system in the basal ganglia. *Trends in neurosciences*, *23*, S28-S33.

Smith, Y., Bennett, B. D., Bolam, J. P., Parent, A., & Sadikot, A. F. (1994). Synaptic relationships between dopaminergic afferents and cortical or thalamic input in the sensorimotor territory of the striatum in monkey. *Journal of Comparative Neurology*, *344*(1), 1-19.

Smith, Y., Villalba, R. M., & Raju, D. V. (2009). Striatal spine plasticity in Parkinson's disease: pathological or not?. *Parkinsonism & related disorders*, *15*,S156-S161.

Song, C. H., Bernhard, D., Bolarinwa, C., Hess, E. J., Smith, Y., & Jinnah, H. A.(2013). Subtle microstructural changes of the striatum in a DYT1 knock-in mouse model of dystonia. *Neurobiology of disease*, *54*, 362-371.

Song, C. H., Fan, X., Exeter, C. J., Hess, E. J., & Jinnah, H. A. (2012). Functional analysis of dopaminergic systems in a DYT1 knock-in mouse model of dystonia. *Neurobiology of disease*, *48*(1), 66-78.

Spacek, J., & Harris, K. M. (2004). Trans-endocytosis via spinules in adult rat hippocampus. *Journal of Neuroscience*, *24*(17), 4233-4241.

Staal, R. G., Mosharov, E. V., & Sulzer, D. (2004). Dopamine neurons release transmitter via a flickering fusion pore. *Nature neuroscience*, *7*(4), 341-346.

Sudarsky, L., Plotkin, G. M., Logigian, E. L., & Johns, D. R. (1999). Dystonia as a presenting feature of the 3243 mitochondrial DNA mutation. *Movement disorders: official journal of the Movement Disorder Society*, *14*(3), 488-491.

Sulzer, D., & Edwards, R. (2000). Vesicles: equal in neurotransmitter concentration but not in volume. *Neuron*, *28*(1), 1-9.

Tao-Cheng, J. H., Dosemeci, A., Gallant, P. E., Miller, S., Galbraith, J. A., Winters, C. A., ... & Reese, T. S. (2009). Rapid turnover of spinules at synaptic terminals. *Neuroscience*, *160*(1), 42-50.

Tashiro, Y., Sugimoto, T., Hattori, T., Uemura, Y., Nagatsu, I., Kikuchi, H., & Mizuno, N. (1989). Tyrosine hydroxylase-like immunoreactive neurons in the striatum of the rat. *Neuroscience letters*, *97*(1-2), 6-10.

Threlfell, S., & Cragg, S. J. (2011). Dopamine signaling in dorsal versus ventral striatum: the dynamic role of cholinergic interneurons. *Frontiers in systems neuroscience*, *5*, 11.

Tong, J. J. (2007). Mitochondrial delivery is essential for synaptic potentiation. *The Biological Bulletin*, *212*(2), 169-175.

Tritsch, N. X., Ding, J. B., & Sabatini, B. L. (2012). Dopaminergic neurons inhibit striatal output through non-canonical release of GABA. *Nature*, *490*(7419), 262266.

Uchigashima, M., Ohtsuka, T., Kobayashi, K., & Watanabe, M. (2016). Dopamine synapse is a neuroligin-2–mediated contact between dopaminergic presynaptic and GABAergic postsynaptic structures. *Proceedings of the National Academy of Sciences*, *113*(15), 4206-4211.

Vanni, V., Puglisi, F., Bonsi, P., Ponterio, G., Maltese, M., Pisani, A., & Mandolesi, G. (2015). Cerebellar synaptogenesis is compromised in mouse models of DYT1dystonia. *Experimental neurology*, *271*, 457-467.

Vastagh, C., Gardoni, F., Bagetta, V., Stanic, J., Zianni, E., Giampà, C., ... & Di Luca, M. (2012). N-methyl-D-aspartate (NMDA) receptor composition modulates dendritic spine morphology in striatal medium spiny neurons. *Journal of Biological Chemistry*, *287*(22), 18103-18114.

Verstreken, P., Ly, C. V., Venken, K. J., Koh, T. W., Zhou, Y., & Bellen, H. J. (2005). Synaptic mitochondria are critical for mobilization of reserve pool vesicles at Drosophila neuromuscular junctions. *Neuron*, *47*(3), 365-378.

Villalba, R. M., & Smith, Y. (2011). Differential structural plasticity of corticostriatal and thalamostriatal axo-spinous synapses in MPTP-treated Parkinsonian monkeys. *Journal of Comparative Neurology*, *519*(5), 989-1005.

Villalba, R.M., Pare, J.F., Smith, Y. (2016) Three-Dimensional Electron Microscopy Imaging of Spines in Non-human Primates. In Bocstale, E.J.V. (ed) *Transmission Electron Microscopy Methods for Understanding the Brain.* Springer Science+Business Media, New York, pp. 81-103.

Von Bohlen Und Halbach, O. (2010). Involvement of BDNF in age-dependent alterations in the hippocampus. *Frontiers in aging neuroscience*, *2*, 136.

Wilson BK, Hess EJ. Animal models for dystonia. Mov Disord. 2013 Jun15; 28(7): 982-9. doi: 10.1002/mds.25526. PMID: 23893454; PMCID: PMC3728703.

Yalcin-Cakmakli, G., Rose, S. J., Villalba, R. M., Williams, L., Jinnah, H. A., Hess, E. J., & Smith, Y. (2018). Striatal cholinergic interneurons in a knock-in mouse model of L-DOPA-Responsive dystonia. *Frontiers in systems neuroscience*, *12*,28.

Yokoi, F., Cheetham, C. C., Campbell, S. L., Sweatt, J. D., & Li, Y. (2013). Presynaptic release deficits in a DYT1 dystonia mouse model. *PLoS One*, *8*(8),e72491.

Yokoi, F., Chen, H. X., Dang, M. T., Cheetham, C. C., Campbell, S. L., Roper, S.N., ... & Li, Y. (2015). Behavioral and electrophysiological characterization of Dyt1 heterozygous knockout mice. *PloS one*, *10*(3), e0120916.

Yokoi, F., Dang, M. T., & Li, Y. (2012). Improved motor performance in Dyt1 ΔGAG heterozygous knock-in mice by cerebellar Purkinje-cell specific Dyt1 conditional knocking-out. *Behavioural brain research*, *230*(2), 389-398.

Yokoi, F., Dang, M. T., Mitsui, S., Li, J., & Li, Y. (2008). Motor deficits and hyperactivity in cerebral cortex-specific Dyt1 conditional knockout mice. *Journal of biochemistry*, *143*(1), 39-47.

Yokoi, F., Oleas, J., Xing, H., Liu, Y., Dexter, K. M., Misztal, C., ... & Li, Y. (2020). Decreased number of striatal cholinergic interneurons and motor deficits in dopamine receptor 2-expressing-cell-specific Dyt1 conditional knockout mice. *Neurobiology of disease*, *134*, 104638.

Yung, K. K. L., Bolam, J. P., Smith, A. D., Hersch, S. M., Ciliax, B. J., & Levey, A. I. (1995). Immunocytochemical localization of D1 and D2 dopamine receptors in the basal ganglia of the rat: light and electron microscopy. *Neuroscience*, *65*(3),709-730.

Zhang, B., Koh, Y. H., Beckstead, R. B., Budnik, V., Ganetzky, B., & Bellen, H. J. (1998). Synaptic vesicle size and number are regulated by a clathrin adaptor protein required for endocytosis. *neuron*, *21*(6), 1465-1475.

Zhang, L., McCarthy, D. M., Sharma, N., & Bhide, P. G. (2015). Dopamine receptor and Gα (olf) expression in DYT1 dystonia mouse models during postnatal development. *PloS one*, *10*(4), e0123104.

Zhao, Y., DeCuypere, M., & LeDoux, M. S. (2008). Abnormal motor function and dopamine neurotransmission in DYT1 ΔGAG transgenic mice. *Experimental neurology*, *210*(2), 719-730.

Ziff, E. B. (1997). Enlightening the postsynaptic density. *Neuron*, *19*(6), 1163-1174.

Zoons, E. (2018). *The role of dopamine and serotonin in cervical dystonia*. Ridderp